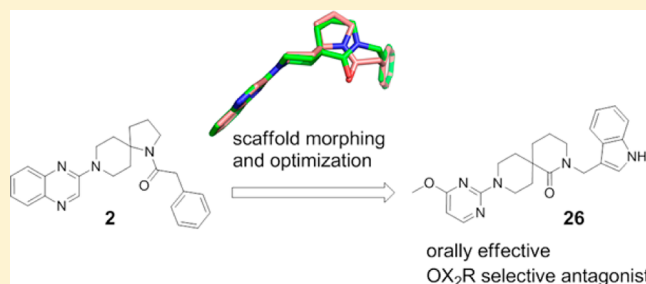


Identification of a Novel Series of Orexin Receptor Antagonists with a Distinct Effect on Sleep Architecture for the Treatment of Insomnia

Claudia Betschart,^{*,†,○} Samuel Hintermann,^{*,†,○} Dirk Behnke,[†] Simona Cotesta,[†] Markus Fendt,^{‡,∞} Christine E. Gee,^{‡,#} Laura H. Jacobson,^{‡,●} Grit Laue,[§] Silvio Ofner,[†] Vinod Chaudhari,^{||,×} Sangamesh Badiger,^{||} Chetan Pandit,^{||} Juergen Wagner,[†] and Daniel Hoyer^{‡,⊥}[†]Global Discovery Chemistry, [‡]Neuroscience, and [§]Metabolism and Pharmacokinetics, Novartis Institutes for BioMedical Research, CH-4002 Basel, Switzerland^{||}Medicinal Chemistry, Aurigene Discovery Technologies, 39-40, Electronic City Phase 2, Bangalore 560 100, India

ABSTRACT: Dual orexin receptor (OXR) antagonists (DORAs) such as almorexant, **1** (SB-649868), or suvorexant have shown promise for the treatment of insomnias and sleep disorders in several recent clinical trials in volunteers and primary insomnia patients. The relative contribution of antagonism of OX₁R and OX₂R for sleep induction is still a matter of debate. We therefore initiated a drug discovery project with the aim of creating both OX₂R selective antagonists and DORAs. Here we report that the OX₂R selective antagonist **26** induced sleep in mice primarily by increasing NREM sleep, whereas the DORA suvorexant induced sleep largely by increasing REM sleep. Thus, OX₂R selective antagonists may also be beneficial for the treatment of insomnia.



■ INTRODUCTION

The orexin system is composed of two widely expressed G-protein-coupled receptors orexin 1 receptor (OX₁R) and orexin 2 receptor (OX₂R) and two peptide agonists orexin A and orexin B (also known as hypocretin 1 and hypocretin 2) that are selectively expressed in a small cluster of neurons in the lateral hypothalamus.^{1,2} The orexin system is involved in a number of systems including feeding, addiction, depression, anxiety, panic, and lung/respiratory function as suggested from animal studies.^{3–6} A key role for the orexin system in the regulation of sleep/wake was indicated by the observations that mice lacking orexin peptides or both orexin receptors display a strong narcoleptic-like phenotype with cataplexy^{7–10} and that familial canine narcolepsy is caused by defective OX₂R signaling.¹¹ Shortly after this discovery, nearly undetectable CSF levels of orexin and the loss or near complete loss of the orexinergic neurons were reported in humans suffering from narcolepsy with cataplexy.^{12,13} Conversely, orexin increases arousal¹⁴ and orexin neurons fire during wake and excite neurons in brain regions important for maintaining wakefulness.^{15–17} Novel treatments for sleep disorders have therefore targeted the orexin system, and the discovery of dual OX₁R/OX₂R as well as subtype selective orexin receptor antagonists has been reported.^{6,18–22} Positive clinical proof of concept studies have demonstrated sleep induction by the three DORAs shown in Figure 1.^{23–27} However, it remains unclear whether targeting one or both receptors is required for sleep induction or conversely if antagonism at both receptors may be detrimental. In mice, loss of OX₁R results in a mild phenotype

with some fragmentation of sleep, whereas mice lacking OX₂R show a more pronounced sleep phenotype albeit milder than that seen with a complete loss of orexin signaling.²⁸ In mice, the sleep inducing properties of the DORA almorexant depend primarily on the presence of OX₂R,²⁹ suggesting that antagonism of OX₂R alone may be sufficient for inducing sleep. Conclusions from experiments using receptor selective antagonists in rats are partially contradictory. Many reports suggest that OX₂R selective antagonists induce sleep, whereas OX₁R selective antagonists are usually reported to lack this effect.^{30–33} Only one group reported on an increase in total sleep time after administration of an OX₁R selective antagonist.³⁴ More controversial is the effect of dual antagonists or coadministration of OX₁R and OX₂R antagonists. While combined antagonism of both receptors was reported to promote less sleep than OX₂R inhibition alone,³¹ it has also been reported that dual antagonism is more effective than antagonism of either receptor alone.³⁴ It is unclear whether variations in time and route of application may be responsible for some of the discrepancy (with the exception of the OX₁R selective antagonist (R)-2-((S)-1-(3,4-dimethoxybenzyl)-6,7-dimethoxy-3,4-dihydroisoquinolin-2(1H)-yl)-N-isopropyl-2-phenylacetamide (ACT335827),³³ application of compounds in these studies was ip, sc, or icv, as properties of the tool compounds did not allow for oral application). Overall, there is strong evidence that at least antagonism of OX₂R is required

Received: May 22, 2013

Published: August 21, 2013

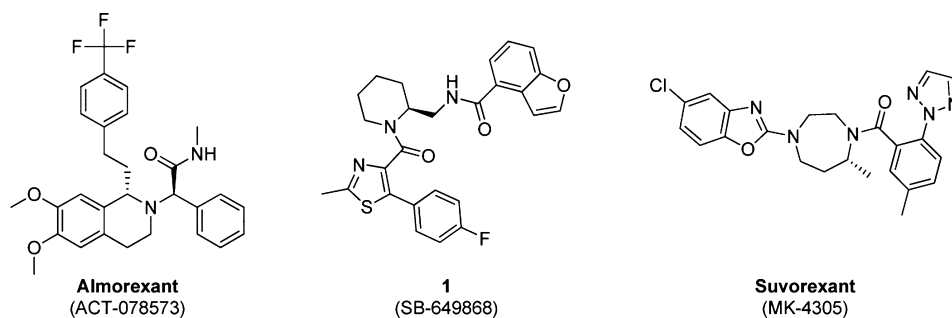
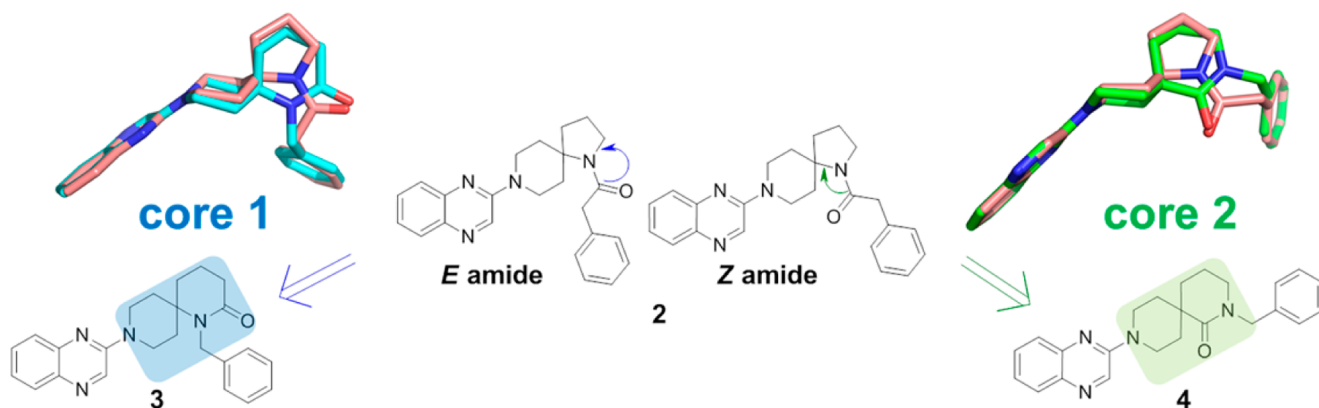
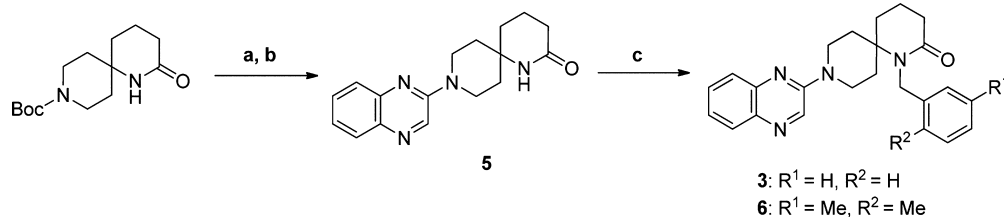


Figure 1. Orexin receptor antagonists in clinical trials.

Scheme 1. Scaffold Morphing of *Z*- and *E*-Amide Conformations of a Literature Compound



Scheme 2. Synthesis of Compounds 3 and 6^a



^aReaction and conditions: (a) TFA, CH₂Cl₂, rt, quant; (b) 2-chloroquinoxaline, K₂CO₃, DMF, 80 °C, 71%; (c) for 3, benzyl bromide, NaH, THF, 60 °C, 19%; for 6, 2,5-dimethylbenzyl chloride, NaH, THF, 60 °C, 22%.

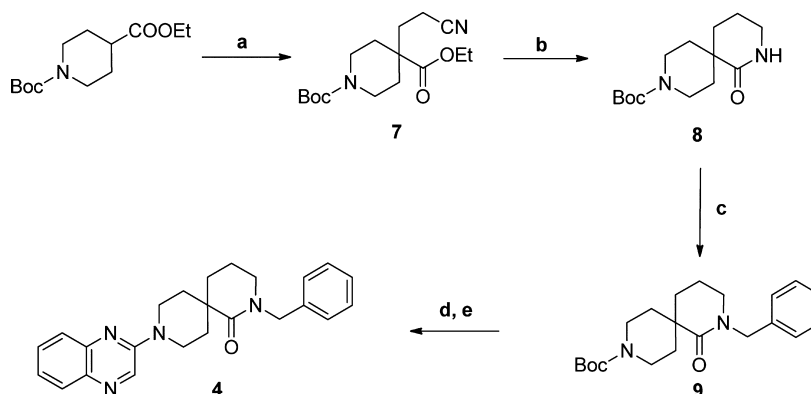
for sleep induction.^{29–37} In our drug discovery program, we sought to generate OX₂R selective antagonists as well as DORAs. Here we present the design of a novel series of orally active orexin receptor antagonists and report on the distinctive effect of an OX₂R selective compound on sleep EEG in mouse, in comparison with the DORA suvorexant.

RESULTS AND DISCUSSION

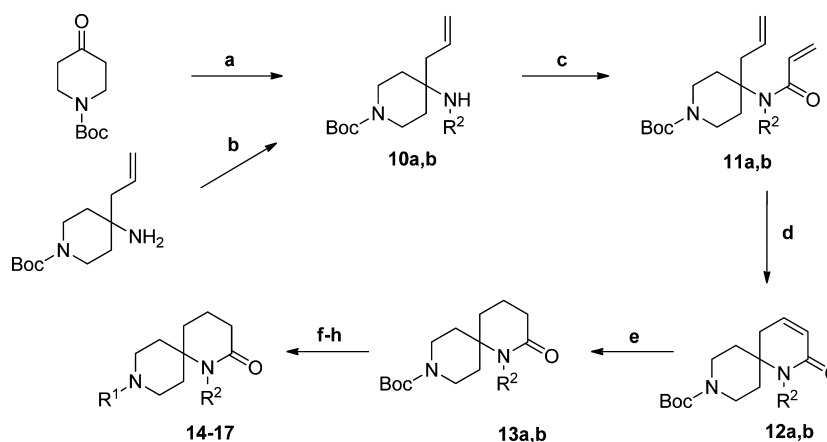
Ligand Design. Analysis of published structures of orexin receptor antagonists revealed in several cases a general motif comprising two aromatic moieties linked by a spacer. In most cases this spacer comprises an aliphatic group and at least one acceptor such as an amide, a urea, or a sulfonamide. For example, in **1** (SB-649868)³⁸ the aromatic elements are the benzofuran and the methylthiazole, and the piperidine is the aliphatic part of the spacer. In suvorexant, the aromatic features are the chlorobenzoxazole and the tolyl, and the diazepane is part of the spacer. To the best of our knowledge, the exact role of the acceptor group has never been clarified. It could be involved in polar interactions with the receptors or may simply be important for constraining a specific ligand conformation.

Therefore, we decided to include this acceptor function in our pharmacophore model. Using this pharmacophore to search our compound library, we identified several novel core structures. Among them were a number of compounds with a carbonyl group as acceptor directly incorporated into the aliphatic group of the spacer. While we decided not to follow up these specific hits, this observation inspired us to apply the same design principle to a spiro scaffold of published orexin antagonists (Scheme 1).^{39,40}

On the basis of our own and published SAR information, we decided to use compound **2**³⁹ as the starting point. Morphing of **2** led to two novel core scaffolds each mimicking either the *E*- or *Z*-configuration of the amide. This is illustrated by the alignments of low energy conformers in Scheme 1. We were expecting to gain some information on the bioactive conformation of **2**, anticipating that only one of the mimics would show potency on the receptors. In order to test our hypothesis, we synthesized compounds **2–4**. The ¹H NMR spectrum of **2** at room temperature showed only one set of resonances, suggesting a fast equilibrium between *E*- and *Z*-amides. Calculations support this interpretation, as the

Scheme 3. Synthesis of Compound 4^a

^aReagents and conditions: (a) (1) LDA, THF, $-78\text{ }^{\circ}\text{C}$; (2) 3-bromopropionitrile, THF, $-78\text{ }^{\circ}\text{C}$ to rt, 40%; (b) Raney Ni, H_2 , NH_3 (5% in EtOH), rt, 41%; (c) NaH, BnBr, TBAI, THF/DMF, $0\text{--}60\text{ }^{\circ}\text{C}$, 67%; (d) 4 M HCl in dioxane, rt, 83%; (e) 2-chloroquinoxaline, NEt_3 , EtOH, microwave, $160\text{ }^{\circ}\text{C}$, 66%.

Scheme 4. Synthesis of Compounds 14–17^a

^aReagents and conditions: (a) (1-tosyl-1H-indol-4-yl)methanamine, 2-allyl-4,4,5,5-tetramethyl-1,3,2-dioxaborolane, toluene, 4 Å molecular sieves, reflux, 70%; (b) 1-tosyl-1H-indole-3-carbaldehyde, 1,2-dichloroethane, AcOH, $60\text{ }^{\circ}\text{C}$, then $\text{NaBH}(\text{OAc})_3$, $60\text{ }^{\circ}\text{C}$, 60%; (c) acryloyl chloride, DIPEA, CH_2Cl_2 , $0\text{ }^{\circ}\text{C}$ to rt, 67–71%; (d) Grubbs second generation catalyst, CH_2Cl_2 , rt, 84–90%; (e) H_2 , 10% Pd/C, MeOH, rt, 96–99%; (f) TFA, CH_2Cl_2 , $0\text{ }^{\circ}\text{C}$ to rt, 95% to quant; (g) R^1Cl , DBU, NMP, $110\text{ }^{\circ}\text{C}$, microwave; (h) Cs_2CO_3 , MeOH, reflux, 20–94% (two steps). Residue R^2 for intermediates 10–13 is defined as follows: (a) (1-tosyl-1H-indol-4-yl)methyl; (b) (1-tosyl-1H-indol-3-yl)methyl.

rotational barrier for the amide is predicted to be around 19 kcal/mol.⁴² Similar observations with respect to *E*- and *Z*-amide rotamers were also reported for other orexin receptor antagonists.^{38,43–47}

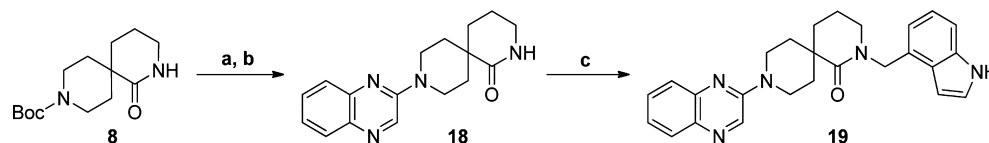
Synthesis. Compounds 3 and 4 were synthesized as described in Schemes 2 and 3. For the *E*-amide mimic 3, synthesis started from commercial 9-boc-1,9-diazaspiro[5.5]undecan-2-one which was deprotected and then reacted with 2-chloroquinoxaline under basic conditions to give the intermediate 5 which was subsequently alkylated with benzyl bromides using sodium hydride as base. By use of 2,5-dimethylbenzyl chloride as alkylating agent, analogue 6 was obtained under the same reaction conditions.

Synthesis of the *Z*-amide mimic 4 first required a reliable access to the spiro-lactam 8 (Scheme 3) that was also necessary for later SAR exploration. Deprotonation of 1-*tert*-butyl 4-ethyl piperidine-1,4-dicarboxylate with LDA at low temperature followed by reaction with 3-bromopropionitrile yielded intermediate 7 reproducibly and in moderate yield. Reduction of the nitrile using Raney nickel as a catalyst under hydrogen atmosphere in ethanolic ammonia yielded the corresponding

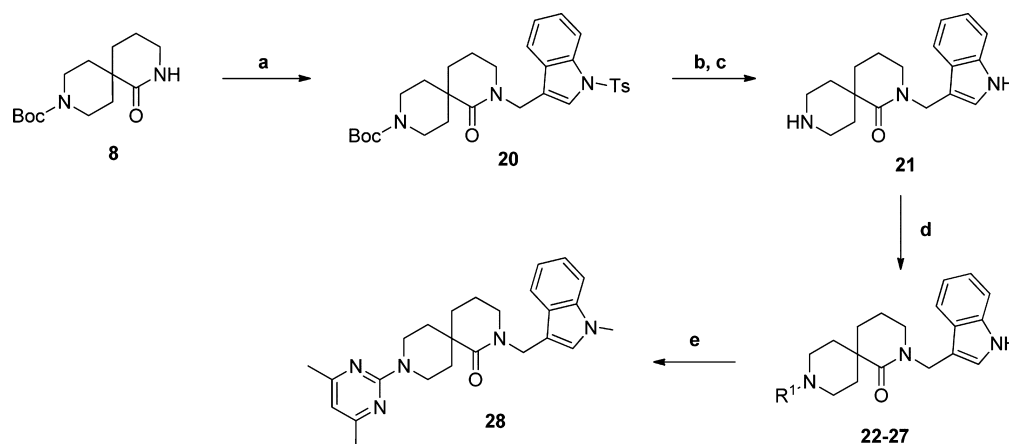
primary amine as intermediate, which cyclized spontaneously to yield the desired lactam 8. Finally, benzoylation of the lactam using sodium hydride as a base followed by Boc deprotection and reaction with 2-chloroquinoxaline gave the desired compound 4 in good yields.

For our initial SAR work around the benzyl group of core 1, we intended to rely on the alkylation strategy that was used for the synthesis of 3. However, it became rapidly evident that alkylation on the rather hindered lactam worked well only for simple and highly reactive alkylating agents such as benzyl bromide. In the case of less reactive reagents, such as indolymethyl halogenides, decomposition of the agents was faster than the desired alkylation and yields were extremely low. In these cases, incorporation of the side chain before closure of the lactam proved to be effective (Scheme 4).

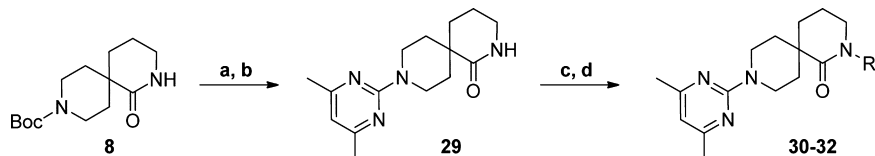
Secondary amines 10 could be synthesized efficiently by two different routes as exemplified in Scheme 4: either by an α -aminoallylation reaction of *N*-boc-piperidine-4-one in a one-pot addition of the allyl group to the in situ generated ketimine using pinacol allylboronate⁴⁸ or by reductive amination of *N*-boc-4-allylpiperidin-4-amine with the corresponding indolylcar-

Scheme 5. Synthesis of Compound 19^a

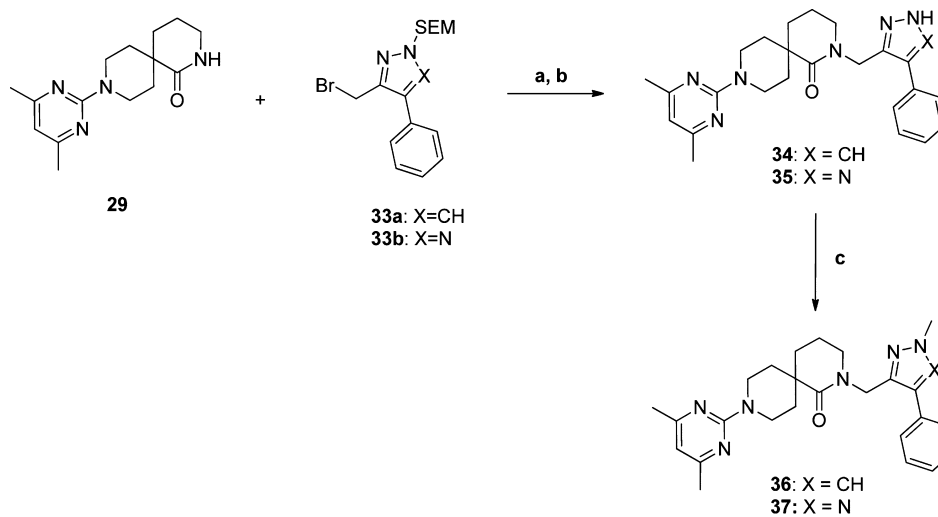
^aReagents and conditions: (a) HCl 4 M in dioxane, CH₂Cl₂, rt, 82%; (b) 2-bromoquinoxaline, K₂CO₃, DMF, 60 °C, 76%; (c) NaH, 4-(bromomethyl)-1-tosyl-1H-indole, THF, 50 °C, 55%.

Scheme 6. Synthesis of Compounds 22–28^a

^aReagents and conditions: (a) LDA, 3-(bromomethyl)-1-tosyl-1H-indole, THF, 0 °C to rt, quant; (b) TFA, CH₂Cl₂, rt, quant; (c) Cs₂CO₃, MeOH, reflux, 99%; (d) R¹-Cl, DIPEA, DBU, MeCN, 120 °C, microwave, 41–74%; (e) NaH, MeI, THF, 0 °C to rt, 25%.

Scheme 7. Synthesis of Compounds 30–32^a

^aReagents and conditions: (a) TFA, CH₂Cl₂, 0 °C to rt, quant; (b) 2-chloro-4,6-dimethylpyrimidine, EtOH, DIPEA, DMAP, 160 °C, microwave, 75%; (c) R²-Br, NaH, TBAI, THF, 0 °C to rt; (d) Cs₂CO₃, MeOH, reflux, 67–88% (two steps).

Scheme 8. Synthesis of Compounds 34–37^a

^aReagents and conditions: (a) NaH, TBAI, THF, 0 °C to rt, (b) 6 M aq HCl, EtOH, 90 °C, 32–91% (two steps); (c) NaH, MeI, THF, 0 °C to rt, 30–74%.

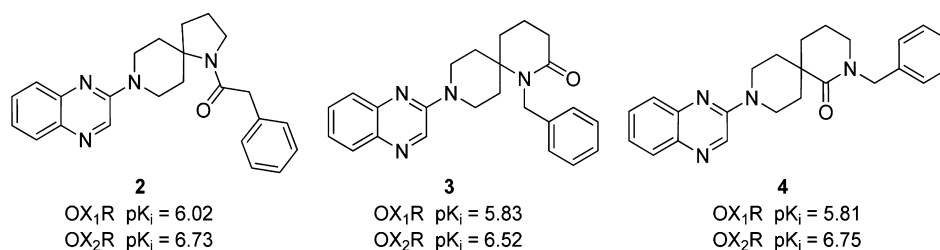


Figure 2. Orexin receptor antagonistic activity of original (**2**) and designed analogous scaffolds (**3** and **4**).

aldehyde. Both routes yielded the desired intermediates **10** in good yields.

Acylation with acryloyl chloride followed by ring-closing metathesis and hydrogenation yielded the substituted lactams **13** in excellent yields. Finally, boc deprotection followed by arylation with the appropriate aryl chlorides under microwave irradiation using cesium carbonate as a base and removal of the tosyl-protecting group led to the final products **14–17**.

For SAR exploration around core **2**, we were delighted to find that the alkylation route worked well for a range of electrophiles. It was found that even the order of the alkylation and the arylation steps was interchangeable, thus allowing incorporation of diversity for both the benzyl and the quinoxalyl portions of the molecule late in the synthesis. Scheme 5 exemplifies the synthesis of the 4-indolyl regioisomer **19** using the arylation/alkylation strategy.

Intermediate **8** was boc-deprotected under acidic conditions and then reacted with 2-bromoquinoxaline in good yield to obtain the desired lactam **18**. Deprotonation of the lactam with sodium hydride and reaction with tosyl-protected 4-(bromomethyl)indole at slightly elevated temperature led to the alkylation product, which under the reaction conditions was also slowly tosyl-deprotected to yield **19**.

Incorporation of a diverse set of quinoxaline replacements, this time using the alkylation/arylation strategy, is exemplified in Scheme 6. The previously described intermediate **8** was alkylated with tosyl protected 3-(bromomethyl)indole using LDA as base. Removal of both protecting groups followed by arylation under microwave irradiation gave direct access to compounds **22–27** in good overall yields. Indole N-alkylation of **27** with iodomethane using sodium hydride as base gave N-methyl analogue **28**.

Synthetic access to substituted indole and indole isosteres is described in Scheme 7. Starting from intermediate **8**, the boc group was removed and the resulting amine reacted with 2-chloro-4,6-dimethylpyrimidine to give the intermediate lactam **29**. Subsequent alkylation using sodium hydride, catalytic amounts of TBAI, and the appropriate alkyl bromides followed by tosyl deprotection using cesium carbonate yielded the respective analogues **30–32**.

Finally, the alkylation strategy was also successfully applied for the introduction of substituted pyrazoles and triazoles on core **2**, as illustrated in Scheme 8. Lactam **29** was reacted with SEM-protected bromides **33** under the same conditions as described in Scheme 7. Then the intermediates were deprotected under acidic conditions to yield the desired compounds **34** and **35**. Methylation under standard conditions gave the corresponding analogues **36** and **37**.

In Vitro SAR. Assuming that only one of the rotamers of **2** would represent the bioactive conformation, we expected a clear difference in potency for the *E*- and *Z*-amide mimics **3** and **4**. To our surprise, the two antagonists showed comparable

potencies on both OX₁R and OX₂R (Figure 2). In addition, the potency was in the same range as for **2**, the analogous example of the original scaffold, thereby validating our design principle.

The similar activity observed for the *E*- and *Z*-amide mimetics **3** and **4** can be interpreted in two ways. Either the carbonyl is not involved in polar interactions with the receptor and its main role is to fix the conformation of the ligand or the two molecules bind to the receptor by different binding modes. In the latter case the carbonyl could be involved in forming polar interactions with different residues.

Initially, we focused our derivatization efforts on **3** (core **1**) mainly because of its more attractive lipophilicity compared to **4** and therefore the resulting favorable lipophilic efficiency (LipE)⁴⁹ (Table 1).

First we investigated the effects of small substituents on the benzyl moiety. A gain in potency by 1 log unit could easily be achieved as exemplified with **6**, however, only at the expense of increased lipophilicity (Table 1). In parallel, we explored heteroaryl replacements of the phenyl group to keep the lipophilicity in a more favorable range. Whereas monoaryl derivatives such as pyridines lost potency (data not shown), some fused biaryls looked promising. For example, the indole moiety reduced lipophilicity in parallel with increased potency (**14** and **15**), resulting in considerably improved ligand efficiency (LE)⁵⁰ and LipE. In particular, the 4-indolyl derivative **15** showed excellent activity, reaching subnanomolar K_i on OX₂R. Next we investigated modifications of the quinoxaline. Interestingly, when the 4-indolyl moiety was kept in place, high potency on OX₂R was retained for a range of substitutions (e.g., **15–17**). On the other hand, activity on OX₁R was more sensitive to structural changes, resulting in some cases in high selectivity for OX₂R (**16**). As we were interested in both OX₂R selective and dual orexin receptor antagonists, the on-target potency optimization was primarily directed toward OX₂R. Nonetheless, the compounds were also routinely tested for antagonism of OX₁R.

With highly potent compounds in hand, *in vivo* characterization was initiated. In mouse PK studies, by use of a cassette dosing approach, very high blood clearances and low absolute oral bioavailabilities were found for all derivatives of core **1**, as exemplified for **15** in Table 2. The investigation of metabolism in liver microsomes or *in vivo* in mice revealed multiple metabolic weak spots. This liability could not be overcome despite major synthetic efforts. Therefore, the focus of optimization was shifted toward derivatives of core **2**, despite their intrinsic higher lipophilicity and lower LipE.

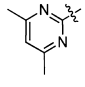
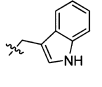
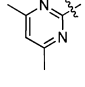
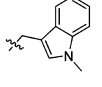
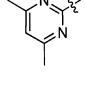
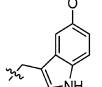
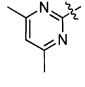
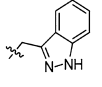
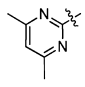
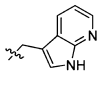
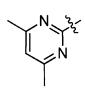
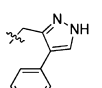
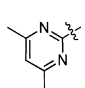
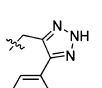
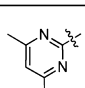
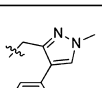
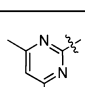
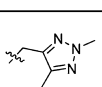
While **3** (*E*-amide mimic) and **4** (*Z*-amide mimic) showed comparable potencies, other modifications revealed clear differences in the SAR for the two cores, supporting the hypothesis that the two scaffolds could adopt different binding modes. It is for instance interesting to note that for core **1**, going from the 3-indolyl derivative **14** to the corresponding 4-

Table 1. In Vitro SAR Data

core 1 **core 2**

comp	core	R ¹	R ²	FLIPR, pK _i ± SEM ^a hOX ₁ R hOX ₂ R		HTlogP ^b	LE OX ₂ R	LipE ^c OX ₂ R
3	1		benzyl	5.83	6.23, 6.81	3.5 ^d	0.32	3.3
4	2		benzyl	5.81 ± 0.03	6.74 ± 0.09	5.5	0.22	1.0
6	1			7.23 ± 0.12	7.89 ± 0.09	4.8	0.36	3.1
14	1			6.70, 6.56	7.16, 7.60	3.9	0.32	3.5
15	1			8.04 ± 0.12	9.34 ± 0.11	3.5	0.42	5.8
16	1			6.43 ± 0.06	9.07 ± 0.09	3.5	0.42	5.6
17	1			7.73 ± 0.06	8.50 ± 0.05	3.3	0.38	5.2
19	2			6.26, 6.39	7.11, 7.31	4.1	0.32	3.1
22	2			6.54 ± 0.04	7.21 ± 0.10	5.1	0.34	2.6
23	2			pIC ₅₀ >5	6.71, 6.51	4.1	0.34	2.5
24	2			pIC ₅₀ >5	6.26, 6.45	3.5	0.32	2.9
25	2			5.85 ± 0.04	7.57 ± 0.05	4.2	0.36	3.4
26	2			6.29 ± 0.06	7.85 ± 0.05	4.9	0.36	3

Table 1. continued

comp	core	R ¹	R ²	FLIPR, pK _i ± SEM ^a		HTlogP ^b	LE OX ₂ R	LipE ^c OX ₂ R
				hOX ₁ R	hOX ₂ R			
27	2			6.18 ± 0.07	8.16 ± 0.09	5.0	0.39	3.2
28	2			5.84 ± 0.07	7.68 ± 0.15	5.5	0.24	2.2
30	2			7.69 ± 0.12	9.78 ± 0.17	5.0	0.42	4.8
31	2			6.31 ± 0.07	8.16 ± 0.19	4.7	0.36	3.5
32	2			5.88 ± 0.13	7.79 ± 0.07	4.6	0.36	3.2
34	2			6.12, 6.11	8.55, 8.41	4.4	0.36	4.1
35	2			6.18, 6.15	8.93 ± 0.14	3.7	0.39	5.2
36	2			6.09 ± 0.05	7.76 ± 0.10	4.2	0.34	3.6
37	2			6.12 ± 0.13	8.34 ± 0.08	4.6	0.35	3.7

^aAverage values from at least three independent measurement. In the cases of $n = 1$ or $n = 2$, individual measurements are reported. ^bSingle measurements (SD of the assay was determined to be 0.34). ^cCalculated using HTlogP (LipE = pK_i - HTlogP). ^dlog P.

Table 2. Mouse PK Data of Selected Compounds^a

compd	intravenous dose, 1 mg/kg ^b		oral dose, 3 mg/kg ^c			
	Cl _{bl} (mL min ⁻¹ kg ⁻¹)	V _{ss} (L/kg)	C _{max,bl} (nM)	AUC _{bl} ^d (nM·h)	F ^e (%)	[br]/[bl] at 15 min pd ± SD ^f
15	188	3.1	18	31	5	0.2 ^g
26	28	1.6	864	2086	47	1.1 ± 0.1

^aThe absorption and disposition parameters were estimated by a noncompartmental analysis of the mean blood concentration ($n = 3$) versus time profile after oral and intravenous administration. ^bDosed as a solution in NMP/blank plasma (10/90, v/v). ^cDosed as a suspension in carboxymethylcellulose 0.5% w/v in water/Tween 80 (99.5%/0.5%, v/v). ^dAUC was extrapolated to infinity. ^eAbsolute oral bioavailability was calculated by dividing the dose-normalized AUC after oral and intravenous dosing assuming linear pharmacokinetics between these two doses. ^fMean brain/blood concentration ratio from $n = 3$. ^gOnly 2 out of 3 animals showed blood or brain levels above the quantitation limit.

indolyl derivative **15** resulted in a potency gain of almost 2 orders of magnitude. This is in contrast to core 2 where no large difference for the corresponding regioisomers **19** and **22** was found. Their potencies were both in the range of the weaker isomer **14** of core 1. Overall, single digit nanomolar

potency for derivatives of core 2 was more difficult to reach than for core 1. Together with the higher lipophilicity, this generally resulted in lower LipE in this series.

Therefore, in an attempt to reduce the lipophilicity, the next round of optimization focused on the quinoxaline part of **22**.

Table 3. Mouse Specific Data for **26** and Suvorexant^a

compd	FLIPR, pK _i ± SEM		[brain] 60 min pd ± SD (pmol/g)	[blood] 60 min pd ± SD (nM)	brain f _u ± SD ^b (%)
	mOX ₁ R	mOX ₂ R			
26	6.34 ± 0.06	7.23 ± 0.04	8778 ± 1205	6912 ± 698	0.61 ± 0.06
suvorexant	8.77 ± 0.14	8.06 ± 0.09	10329 ± 3667	10461 ± 3584	0.65 ± 0.05

^aAll compounds were dosed per os at 50 mg/kg as a suspension in methylcellulose 0.5% w/v in water. Shown are the mean values ($n = 3$) ± SD.

^bThe free fraction in mouse brain homogenate was assessed using a slightly adapted literature method.⁵²

Pyrazine as a monocyclic replacement (**23**) led to the expected reduction of log *P* by 1 unit, albeit at the expense of a lower potency. In the case of the pyrimidine (**24**), lipophilicity reduction was more significant, leading to an increase of LipE by half a unit. In addition, potency could be recovered by appropriate substitution of the pyrimidine. For instance, incorporation of a methyl (**25**) or a methoxy group (**26**) in position 4 or 4,6-dimethyl substitution (**27**) led to increased potencies and a net increase in LipE. A further jump in potency and LipE could be achieved by substitution of the indole 5-position with small lipophilic substituents, as exemplified by methoxy analogue **30**, leading to highly potent OX₂R-preferring antagonists.

N-Methylation of the indole (**28**) led to only a marginal drop in potency, suggesting that the NH is not involved in a direct interaction with the receptors. The corresponding indazole (**31**) and aza-indole (**32**) derivatives were found to be equipotent OX₂R antagonists. As expected, the measured log *P* was lower for the two analogues when compared to **27**.

In a next round of optimization, the indazole was morphed into a 4-phenylpyrazole (this can formally be seen as a ring-opening of the annulated system) leading to analogue **34** which turned out to be a very potent OX₂R antagonist. Interestingly, in contrast to the indole, N-methylation of the phenylpyrazole (**35**) led to a loss of 1 order of magnitude in potency. Finally, when going from the pyrazole to the triazole, a very potent antagonist (**36**) with increased LipE (5.2) was identified. As for the indoles, N-methylation (**37**) had only a small impact on potency but still led to a decrease of LipE. Interestingly, compounds **34–37** contain a biaryl moiety, a common motif in known orexin antagonists (see, for example, **1** and suvorexant), indicating that the core **2** compounds could interact with the receptors through similar interactions.

In Vivo Characterization. Compounds with promising in vitro properties were tested for their blood pharmacokinetic and brain penetration properties in mice. A cassette dosing setup was applied; i.e., five experimental compounds and a reference compound were administered together intravenously at 1 mg/kg and per os at 3 mg/kg. The exposure in blood after oral administration mainly appeared to be driven by blood clearance. In particular, **26** that had low blood clearance (see Table 2) showed high maximal blood exposure and AUC after oral dosing. It exhibited an acceptable absolute oral bioavailability and a brain/blood concentration ratio that indicated favorable brain penetration. On the basis of the overall properties, **26** was selected for testing its pharmacological activity in mice.

For a comprehensive interpretation of the in vivo data, the potencies of **26** and suvorexant were determined at the mouse orexin receptors (mOX₁R, mOX₂R) in a functional assay (Table 3).⁵¹ Suvorexant was found to be slightly selective for mOX₁R over mOX₂R, whereas **26** showed a 10-fold preference for mOX₂R (Table 3).

A locomotor activity assay in mouse was used as a filter before performing more resource demanding sleep measurements. In addition, brain and blood levels were determined 1 h postdose in satellite groups of animals (Table 3). In the locomotor paradigm, reduction of motility (i.e., increase in inactivity) was measured as a surrogate for sleep.⁵³ Animals were dosed orally immediately before lights off (start of the active phase). Inactivity was defined as at least 1 min with no infrared beam breaks. The increase in inactivity during the first 4 h postdose was calculated relative to the same 4 h on the previous day during the habituation phase.²⁹ Suvorexant was used as positive control. Dosed at 50 mg/kg, **26** and suvorexant had a significant effect in this model (Figure 3). Estimated free

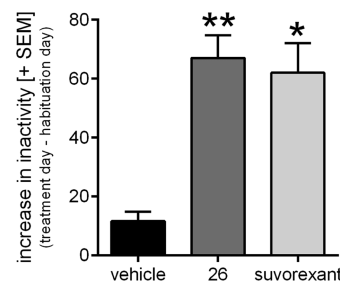


Figure 3. Effect of **26** and suvorexant in the locomotor paradigm (increase of inactivity [min] in the 4 h following application). Both compounds were administered at a dose of 50 mg/kg ($n = 6$): (*) $p < 0.05$, (**) $p < 0.01$ one-way ANOVA with post hoc Dunnett's tests (comparison with vehicle).

levels of compound in the brain were calculated by multiplying the fraction unbound as measured in a separate mouse brain homogenate assay with the brain levels of compound achieved in a satellite group. The data suggested that both compounds were present at similar levels to interact with orexin receptors in the brain (Table 3). These levels of both compounds were high enough to reach the maximal achievable increase in inactivity during the first 4 h. Because of its significant activity in the locomotor paradigm, **26** was selected for studying the effects on mouse sleep.

The effect of orexin receptor antagonists on sleep in mice was determined by EEG (electrocorticogram/electroencephalogram) and EMG (electromyogram) recordings. Freely moving C57Bl/6 mice with chronically implanted electrodes were well habituated to the experiment boxes and had access to food and water ad libitum. The test compounds or vehicle were administered per os as a suspension in 0.5% methylcellulose immediately prior to lights off (start of the active phase) and start of recording. Movement was recorded using infrared sensors in the roof of the box. EEG/EMG signals and motility data were used to score 10 s epochs into wake, NREM sleep, and REM sleep. Each animal served as its own control by application and recording of vehicle the day before compound dosing.

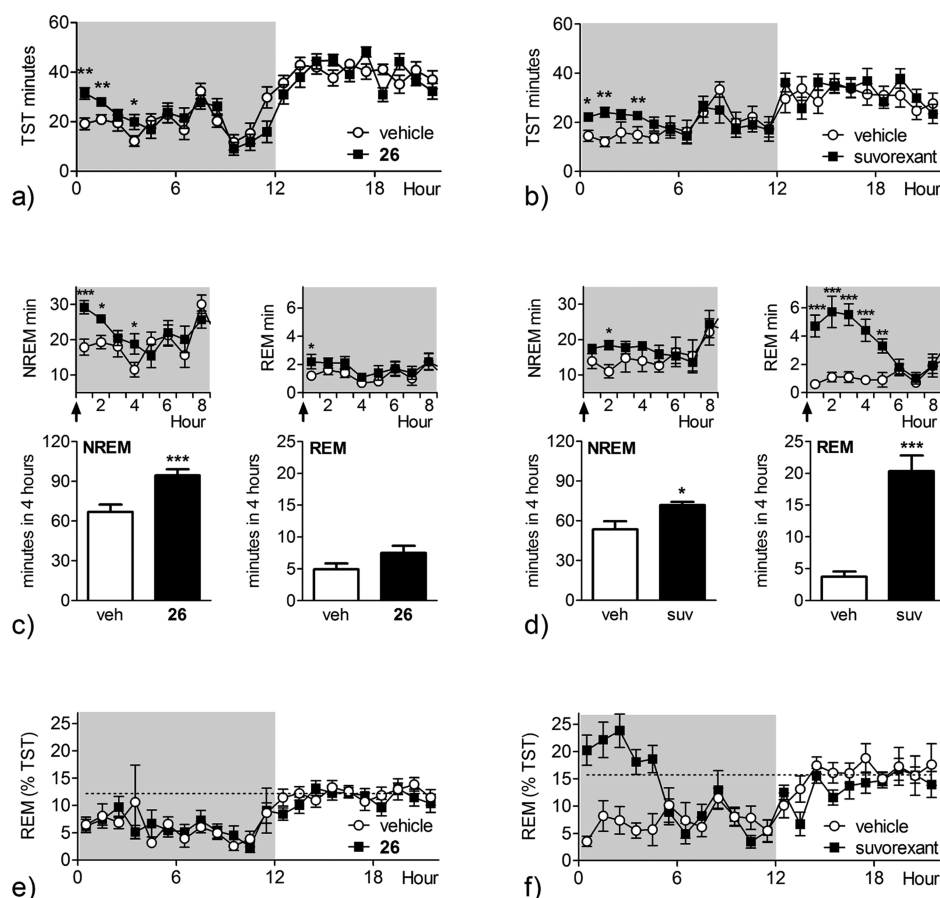


Figure 4. Sleep induction by **26** and suvorexant. (a, b) Vehicle or compounds were dosed just before lights off (hour 0) in a crossover design, and total sleep time (TST) increased during the first 4 h with both compounds (**26**, $n = 11$; suvorexant, $n = 10$). (c, d) Amount of NREM and REM sleep during the first hours after lights off and quantified during the first four hours. (e, f) REM proportion of total sleep time. Dotted line indicates the mean proportion on the vehicle day during the inactive (lights on) phase. Shading indicates lights off. Time course graphs: (*) $p < 0.05$; (**) $p < 0.01$; (***) $p < 0.001$; Fisher's LSD. Bar graphs: (*) $p < 0.05$; (**) $p < 0.01$; (***) $p < 0.001$; paired t test.

The effect of **26** and suvorexant both at 50 mg/kg po were compared. Both compounds showed a fast onset of action, with a clear increase in total sleep time during the first hour after dosing (Figure 4a,b). The effect lasted 4–5 h, after which time the total sleep time per hour was the same as on vehicle day. The increase in total sleep time during the first four hours was in a similar range for both compounds, despite the fact that the apparent free brain levels in relation to the potency on the orexin receptors were much higher for suvorexant than for **26** (Table 3). Analysis of the sleep architecture revealed a surprising difference between the two compounds. Suvorexant induced a very strong increase in REM sleep, which accounted for much of the increase in total sleep time (Figure 4d). Suvorexant also increased NREM sleep during the first four hours but to a lesser extent. This was in sharp contrast to **26**, which primarily increased sleep by a strong effect on NREM sleep, accompanied by a smaller increase in REM sleep that was not significant following the first hour (Figure 4c). When the same data were used to examine the percentage of total sleep time spent in REM, treatment with **26** did not change the balance between REM and NREM sleep (Figure 4e), whereas treatment with suvorexant dramatically increased the proportion of REM sleep to levels considerably higher than the mean level during normal sleep in the inactive period (Figure 4f).

These findings are particularly interesting in connection with recently published data from clinical trials with suvorexant and

other DORAs in both healthy subjects and in patients suffering from primary insomnia.^{27,54} Despite the fact that mice show a very distinct sleep behavior compared to humans (nocturnal activity, more fragmented sleep pattern), the observations in this species appear to be quite predictive of the effects seen in humans. As described above, in mice suvorexant induced a strong increase in REM sleep, accounting for around half of the increase in total sleep time. In patients suffering from insomnia, about half of the increase in total sleep time due to suvorexant was attributable to an increase in time spent in REM and when the percentage of total sleep time spent in a particular sleep stage was analyzed, only REM sleep showed a nominally significant increase versus placebo for all tested doses (10–80 mg).⁵⁴ Similarly, in healthy subjects suvorexant increased sleep with about half the increase attributable to an increase in time spent in REM sleep.²⁷ An earlier report on a clinical study with **1** revealed similar effects of this DORA, with a very strong increase in REM sleep and at the highest dose the appearance of sleep onset REM periods.⁵⁵ Whether the difference in selectivity for OX₁R and OX₂R is the key explanation for the distinctive architecture of the sleep induced by **26** can currently only be speculated. Interestingly, mouse sleep induced by almorexant also has a very different architecture than sleep induced by suvorexant and is not accompanied by an overproportional increase in REM.²⁹ However, while almorexant is generally considered a DORA, it has the property that the

relative affinity for OX₂R increases with time because of its very slow dissociation from OX₂R,^{29,56,57} suggesting it may behave in vivo more like an OX₂R preferring antagonist.

Animal experiments applying selective or dual orexin receptor antagonists have produced somewhat contradictory conclusions regarding the importance of antagonizing OX₁R and OX₂R for sleep induction and architecture.^{29–32,34,35} Intracerebroventricular injection of the OX₂R antagonist (S)-1-(6,7-dimethoxy-3,4-dihydroisoquinolin-2(1H)-yl)-3,3-dimethyl-2-((pyridin-4-ylmethyl)amino)butan-1-one hydrochloride (TCS-OX2-29) increased REM, at odds with our results.³² On the other hand, addition of an OX₁R antagonist to an OX₂R antagonist further decreased latency to REM, while suppressing both the decrease in latency and increase in NREM produced by OX₂R antagonism is in line with our results³¹ as are the effects of OX₁R knockdown in locus coeruleus³⁷ and ip application of 1-(2-methylbenzoxazol-6-yl)-3-[1,5]-naphthyridin-4-ylurea hydrochloride (SB-334867-A).³⁵ Differences in experimental design, properties of the compounds, and the species used make it difficult to determine the extent to which receptor selectivity, rather than other factors, accounts for the observed differences in sleep architecture. What is clear is that antagonism of OX₂R is sufficient to promote sleep in rodents. At present, no clinical data using a selective OX₂R antagonist have been published. When such data become available, they will be important for further understanding how the sleep profile found in rodents translates to humans and whether or not OX₂R is a superior target for the treatment of insomnia in man.

In conclusion, two novel series of orexin receptor antagonists were designed based on a pharmacophore analysis of published orexin receptor antagonists. They mimic two potential low energy conformations of known spiro-type orexin receptor antagonists. Representative compounds of core 2 showed a good overall profile supporting in vivo testing. **26**, an OX₂R selective antagonist, was chosen for comparison with the dual antagonist suvorexant in mouse sleep studies. Suvorexant and **26** both induced sleep in mice. While suvorexant mainly increased REM sleep in this model, the balance between NREM and REM sleep was preserved under **26**. Our studies demonstrate that selective OX₂R antagonists may be a viable alternative to DORAs for the treatment of insomnia, with the potential to induce sleep without strongly increasing the REM component. Whether these distinct effects are linked to differences in the selectivity profile for the two orexin receptors requires further study. The translatability of rodent sleep architecture to human sleep will be better understood after OX₂R selective compounds are tested in the clinic.

■ EXPERIMENTAL SECTION

A. Chemistry. All reagents and solvents were purchased from commercial suppliers and used without further purification or were prepared according to published procedures. All reactions were performed under inert conditions (argon) unless otherwise stated. ¹H NMR spectra were recorded on a Bruker 400 MHz or a Bruker 600 MHz NMR spectrometer. Chemical shifts are reported in parts per million (ppm) relative to an internal solvent reference. Significant peaks are tabulated in the order multiplicity (s, singlet; d, doublet; t, triplet; q, quartet; quintet; m, multiplet; br, broad), coupling constants, and number of protons. Final compounds were purified to ≥95% purity as assessed by analytical liquid chromatography with one of the following methods.

Method A: Waters Acquity UPLC–MS; column HSS T3 1.8 μm, 2.1 mm × 50 mm; A, water + 0.05% formic acid + 3.75 mM ammonium

acetate; B, acetonitrile + 0.04% formic acid; 2–98% B in 1.4 min, 98% B 0.45 min, flow 1.2 mL/min; column temperature 50 °C.

Method B: Agilent 1100 series; LC–MS; column Zorbax SB-C18 1.8 μm, 3.0 mm × 30 mm; A, water + 0.05% trifluoroacetic acid; B, acetonitrile + 0.05% trifluoroacetic acid; 30–100% B in 3.25 min, 100% B 0.75 min; flow 0.7 mL/min; column temperature 35 °C.

Method C: Agilent 1100 series; Agilent MSD vs1 single quad mass spectrometer; column Mercury MS Synergi 2 μm, 20 mm × 4.0 mm; A, water + 0.1% formic acid; B, acetonitrile; 30–95% B in 1.5 min, 95% B 1 min; flow 2.0 mL/min; column temperature 30 °C.

Method D: Agilent 1100 series; LC–MS; column Zorbax SB-C18 1.8 μm, 3.0 mm × 30 mm; A, water + 0.05% trifluoroacetic acid; B, acetonitrile + 0.05% trifluoroacetic acid in; 10–100% B in 3.25 min, 100% B in 0.75 min; flow 0.7 mL/min; column temperature 35 °C.

The accurate mass analyses were performed by using electrospray ionization in positive mode after separation by liquid chromatography. The elemental composition was derived from the averaged mass spectra acquired at a high resolution of about 30 000 on an LTQ Orbitrap XL mass spectrometer (Thermo Scientific). The high mass accuracy below 1 ppm was obtained by using a lock mass.

1-Benzyl-9-(quinoxalin-2-yl)-1,9-diazaspiro[5.5]undecan-2-one (3). NaH (34.8 mg, 0.871 mmol, 60% in mineral oil) was added to an ice-cold solution of 9-(quinoxalin-2-yl)-1,9-diazaspiro[5.5]undecan-2-one (**5**) (86 mg, 0.29 mmol) in THF (5 mL), and the suspension was stirred for 1 h at 0 °C. Then benzyl bromide (64.5 mg, 0.377 mmol) was added at 0 °C, and the reaction mixture was allowed to warm to room temperature and stirred for 24 h. The mixture was poured into water, and the solution was extracted twice with ethyl acetate. The combined organic layers were washed with water and brine, filtered, and dried over anhydrous sodium sulfate. The organic layer was concentrated under reduced pressure. The crude product was purified by flash column chromatography (dichloromethane/methanol 97:3) to yield the title compound **3** (24 mg, 19%). ¹H NMR (400 MHz, DMSO-*d*₆) δ ppm 8.78 (s, 1H), 7.79 (d, *J* = 8.07 Hz, 1H), 7.55 (d, *J* = 4.16 Hz, 2H), 7.36 (ddd, *J* = 3.55, 4.83, 8.25 Hz, 1H), 7.18–7.27 (m, 2H), 7.04–7.17 (m, 3H), 4.39–4.62 (m, 4H), 3.09 (t, *J* = 12.35 Hz, 2H), 2.41 (t, *J* = 6.60 Hz, 2H), 2.03–2.16 (m, 2H), 1.96 (dt, *J* = 4.52, 12.90 Hz, 2H), 1.72–1.86 (m, 2H), 1.52–1.67 (m, 2H). HRMS (ESI⁺) calcd for C₂₄H₂₇N₄O (MH⁺) 387.217 60, found 387.217 94. UPLC–MS *t*_{R,A} = 1.07 min, [M + H]⁺ = 387.4.

2-Benzyl-9-(quinoxalin-2-yl)-2,9-diazaspiro[5.5]undecan-1-one (4). To a solution of *tert*-butyl 2-benzyl-1-oxo-2,9-diazaspiro[5.5]undecane-9-carboxylate (**9**) (440 mg, 1.20 mmol) in dichloromethane (5 mL) was added 4 M HCl in dioxane (10 mL). The solution was stirred for 18 h at room temperature. After completion of the reaction the mixture was evaporated to dryness. The residue was crystallized from THF/heptane 3:1 to yield 2-benzyl-2,9-diazaspiro[5.5]undecan-1-one hydrochloride as white crystals (293 mg, 83%).

To the solution of 2-benzyl-2,9-diazaspiro[5.5]undecan-1-one hydrochloride (100 mg, 0.34 mmol) in ethanol (1 mL) in a microwave tube were added 2-chloroquinoxaline (95 mg, 0.58 mmol) and triethylamine (0.14 mL, 1.02 mmol). The tube was sealed, and the reaction mixture was heated at 160 °C for 15 min under microwave conditions. The solvent was removed under reduced pressure. The resulting crude product was purified by flash column chromatography (hexane/ethyl acetate 2:1) to yield the title compound **4** (114 mg, 66%). ¹H NMR (600 MHz, DMSO-*d*₆) δ ppm 8.84 (s, 1H), 7.81 (d, *J* = 8.07 Hz, 1H), 7.53–7.63 (m, 2H), 7.36–7.41 (m, 1H), 7.34 (t, *J* = 7.57 Hz, 2H), 7.22–7.29 (m, 1H), 7.19 (d, *J* = 7.27 Hz, 2H), 4.50 (s, 2H), 4.24–4.34 (m, 2H), 3.39–3.49 (m, 2H), 3.22 (t, *J* = 6.26 Hz, 2H), 2.01–2.15 (m, 2H), 1.86–1.93 (m, 2H), 1.73–1.84 (m, 2H), 1.55–1.66 (m, 2H). HRMS (ESI⁺) calcd for C₂₄H₂₇N₄O (MH⁺) 387.217 94, found 387.218 16. LC–MS *t*_{R,D} = 3.29 min, [M + H]⁺ = 387.2.

9-(Quinoxalin-2-yl)-1,9-diazaspiro[5.5]undecan-2-one (5). To a solution of *tert*-butyl 2-oxo-1,9-diazaspiro[5.5]undecane-9-carboxylate [1031927-12-4] (920 mg, 3.26 mmol) in dichloromethane (10 mL) was added TFA (2.53 mL, 32.6 mmol). The solution was stirred for 40 min at room temperature. The mixture was evaporated

under reduced pressure and dried under high vacuum to yield 1,9-diazaspiro[5.5]undecan-2-one trifluoroacetate (1.90 g, 100%). ¹H NMR (400 MHz, DMSO-*d*₆) δ ppm 8.59–8.35 (m, 2H), 7.83 (s, 1H), 3.27–3.14 (m, 2H), 3.12–2.98 (m, 2H), 2.17–2.04 (m, 2H), 1.80–1.57 (m, 8H); UPLC–MS *t*_{R,A} = 0.20 min, [M + H]⁺ = 169.2.

To a stirred solution of 1,9-diazaspiro[5.5]undecan-2-one trifluoroacetate (800 mg, 4.76 mmol) in 10 mL of DMF were added 2-chloroquinoxaline (937 mg, 5.71 mmol) and K₂CO₃ (3.3 g, 23.8 mmol), and the reaction mixture was stirred for 18 h at 80 °C under a nitrogen atmosphere. The reaction mixture was quenched with ice-cold water and extracted with ethyl acetate (2 × 50 mL), dried over anhydrous Na₂SO₄, filtered, and concentrated under reduced pressure. The crude mixture was purified by flash column chromatography (3% methanol in chloroform) to yield the title compound **5** (1.0 g, 71%). ¹H NMR (400 MHz, DMSO-*d*₆) δ ppm 8.83 (s, 1H), 7.79 (d, *J* = 8.07 Hz, 1H), 7.50–7.64 (m, 3H), 7.30–7.42 (m, 1H), 4.12 (td, *J* = 4.86, 13.75 Hz, 2H), 3.46–3.63 (m, 2H), 2.12 (t, *J* = 6.11 Hz, 2H), 1.54–1.82 (m, 8H). UPLC–MS *t*_{R,A} = 0.79 min, [M + H]⁺ = 297.3.

1-(2,5-Dimethylbenzyl)-9-(quinoxalin-2-yl)-1,9-diazaspiro[5.5]undecan-2-one (6). To a solution of 9-(quinoxalin-2-yl)-1,9-diazaspiro[5.5]undecan-2-one (**5**) (80 mg, 0.27 mmol) in THF (5 mL) was added NaH 95% (32 mg, 0.81 mmol), and the mixture was stirred for 10 min at room temperature. Then 2,5-dimethylbenzyl chloride (70 mg, 0.35 mmol) was added, and the reaction mixture was heated at 60 °C for 18 h. Saturated aqueous NH₄Cl solution (40 mL) was added, and the reaction mixture was extracted with ethyl acetate (100 mL). The organic layer was dried over Na₂SO₄, filtered, and concentrated under reduced pressure. The resulting crude product was purified by reversed phase preparative HPLC (column Zorbax eclipseXDB C18, flow 20 mL/min, mobile phase 0.1% TFA in water (A), acetonitrile (B) gradient) to yield the title compound **6** (49 mg, 22%). ¹H NMR (400 MHz, DMSO-*d*₆) δ ppm 8.78 (s, 1H), 7.78 (d, *J* = 7.82 Hz, 1H), 7.51–7.59 (m, 2H), 7.36 (ddd, *J* = 2.57, 5.81, 8.25 Hz, 1H), 6.90–6.95 (m, 1H), 6.82–6.88 (m, 1H), 6.69 (s, 1H), 4.48 (d, *J* = 12.96 Hz, 2H), 4.34 (s, 2H), 3.11 (t, *J* = 12.10 Hz, 2H), 2.42 (t, *J* = 6.60 Hz, 2H), 2.21 (s, 3H), 2.09–2.19 (m, 2H), 2.04 (s, 3H), 1.77–1.97 (m, 4H), 1.66 (d, *J* = 13.20 Hz, 2H). HRMS (ESI⁺) calcd for C₂₆H₃₁N₄O (MH⁺) 415.249 53, found 415.249 24. UPLC–MS *t*_{R,A} = 1.18 min, [M + H]⁺ = 415.3.

1-tert-Butyl 4-Ethyl 4-(2-cyanoethyl)piperidine-1,4-dicarboxylate (7). To a solution of ethyl *N*-boc-piperidine-4-carboxylate [124443-68-1] (10.0 g, 38.86 mmol) in THF (200 mL) was added LDA (2 M solution in hexane, 38.86 mL, 77.72 mmol) at –78 °C, and the mixture was stirred for 30 min. Then 3-bromopropionitrile (6.25 g, 46.63 mmol) was added at –78 °C. The resulting reaction mixture was stirred at –60 °C for 4 h and quenched with saturated NH₄Cl solution. Ethyl acetate was added, and the organic layer was washed with water and brine. The organic layer was dried over Na₂SO₄, filtered, and concentrated. The crude product was purified by column chromatography using 10% ethyl acetate in hexane to yield the title compound **7** as a pale yellow liquid (5.0 g, 40%). ¹H NMR (400 MHz, DMSO-*d*₆) δ ppm 4.08–4.16 (m, 2H), 3.60–3.77 (m, 2H), 2.82 (br s, 2H), 2.41 (t, *J* = 7.62 Hz, 2H), 1.87–1.96 (m, 2H), 1.82 (t, *J* = 7.82 Hz, 2H), 1.26–1.40 (m, 11H), 1.19 (t, *J* = 7.62 Hz, 3H). UPLC–MS *t*_{R,A} = 1.07 min, [M + H]⁺ = 311.3.

tert-Butyl 1-Oxo-2,9-diazaspiro[5.5]undecane-9-carboxylate (8). A suspension of Raney Ni (5.0 g) in ethanolic ammonia (~20% v/v) and 1-tert-butyl 4-ethyl 4-(2-cyanoethyl)piperidine-1,4-dicarboxylate (**7**) (8.5 g, 27.42 mmol) was hydrogenated at 100 psi for 48 h at room temperature in an autoclave. After completion of the reaction, the catalyst was filtered off and washed with ethanol. The combined filtrate was concentrated under reduced pressure and triturated with *n*-pentane to yield a solid which was purified by column chromatography (6% methanol in chloroform) to furnish the title compound **8** as a white solid (3.0 g, 41%). ¹H NMR (400 MHz, DMSO-*d*₆) δ ppm 7.31 (br s, 1H), 3.65 (td, *J* = 4.25, 13.39 Hz, 2H), 2.92–3.11 (m, 4H), 1.72–1.84 (m, 2H), 1.58–1.72 (m, 4H), 1.37 (s, 9H), 1.26–1.35 (m, 2H). LC–MS *t*_{R,D} = 2.889 min, [M + H]⁺ = 269.1.

tert-Butyl 2-Benzyl-1-oxo-2,9-diazaspiro[5.5]undecane-9-carboxylate (9). NaH (64.4 mg, 2.68 mmol) was added to an ice-

cold solution of *tert*-butyl 1-oxo-2,9-diazaspiro[5.5]undecane-9-carboxylate (**8**) (480 mg, 1.79 mmol) in THF (3 mL). The resulting mixture was stirred at 0 °C for 10 min, and TBAI (66.1 mg, 0.18 mmol) was added. Then benzyl bromide (0.32 mL, 2.68 mmol) was added at 0 °C, and the reaction mixture was allowed to warm to room temperature and heated at 45 °C for 20 h. The mixture was poured into water, and the solution was extracted twice with ethyl acetate. The combined organic layers were washed with water and brine, filtered, and dried over anhydrous sodium sulfate. The organic layer was concentrated under reduced pressure. The crude product was purified by flash column chromatography (hexane/ethyl acetate 2:1) to yield the title compound **9** (440 mg, 67%). ¹H NMR (400 MHz, DMSO-*d*₆) δ ppm 7.28–7.35 (m, 2H), 7.19–7.26 (m, 1H), 7.15 (d, *J* = 7.04 Hz, 2H), 4.46 (s, 2H), 3.58–3.78 (m, 2H), 3.16 (t, *J* = 5.87 Hz, 2H), 3.02 (br s, 2H), 1.82–1.94 (m, 2H), 1.65–1.81 (m, 4H), 1.31–1.46 (m, 11H).

tert-Butyl 4-Allyl-4-((1-tosyl-1H-indol-4-yl)methylamino)piperidine-1-carboxylate (10a). To a stirred mixture of 1-boc-piperidin-4-one [79099-07-3] (0.25 g, 1.256 mmol), 4 Å molecular sieves (0.25 g), and allyl boronic acid pinacol ester (0.255 g, 1.507 mmol) in toluene (10 mL) was added 1-tosyl-1H-indol-4-yl-methanamine (0.45 g, 1.507 mmol), and the reaction mixture was heated at reflux for 16 h. The mixture was filtered through a pad of Celite. The filtrate was concentrated under reduced pressure and the residue was purified by column chromatography (10% ethyl acetate in hexane) to yield the title compound **10a** as a white solid (0.2 g, 70%). LC–MS *t*_{R,C} = 0.341 min, [M + H]⁺ = 524.0.

tert-Butyl 4-Allyl-4-((1-tosyl-1H-indol-3-yl)methylamino)piperidine-1-carboxylate (10b). To a solution of 1-tosyl-1H-indole-3-carbaldehyde [50562-79-3] (1.90 g, 6.35 mmol) in 1,2-dichloroethane (30 mL) were added *tert*-butyl 4-allyl-4-amino-piperidine-1-carboxylate⁵⁸ (1.52 g, 6.35 mmol) and acetic acid (381 mg, 6.35 mmol). The resulting solution was heated at 60 °C for 3 h. Then NaBH(OAc)₃ was added, and the reaction mixture was heated at 60 °C for 38 h. The mixture was cooled to room temperature. Saturated NaHCO₃ solution (30 mL) was added and extracted with ethyl acetate (3 × 50 mL). The combined organic layers were washed with water and brine, then dried over anhydrous Na₂SO₄, filtered, and concentrated under reduced pressure. The crude mixture was purified by flash column chromatography (20% ethyl acetate/hexane) to yield the title compound **10b** (2.0 g, 60%). LC–MS *t*_{R,C} = 0.34 min, [M + H]⁺ = 524.0.

tert-Butyl 4-Allyl-4-(N-((1-tosyl-1H-indol-4-yl)methyl)acrylamido)piperidine-1-carboxylate (11a). Acryloyl chloride (0.360 g, 0.401 mmol) was added at 0 °C to a stirred solution of *tert*-butyl 4-allyl-4-((1-tosyl-1H-indol-4-yl)methylamino)piperidine-1-carboxylate (**10a**) (0.2 g, 0.382 mmol) and diisopropylethylamine (0.32 mL, 1.91 mmol) in dichloromethane (5.0 mL). The reaction mixture was stirred at 0 °C for 30 min and was then allowed to warm to room temperature and stirred for 4 h. The reaction mixture was concentrated under reduced pressure and the crude product was purified by column chromatography (5% ethyl acetate in hexane) to yield the title compound **11a** as a white solid (0.16 g, 72%). LC–MS *t*_{R,C} = 0.774 min, [M + H – boc]⁺ = 477.9.

tert-Butyl 2-Oxo-1-((1-tosyl-1H-indol-4-yl)methyl)-1,9-diazaspiro[5.5]undec-3-ene-9-carboxylate (12a). To a solution of *tert*-butyl 4-allyl-4-(N-((1-tosyl-1H-indol-4-yl)methyl)acrylamido)piperidine-1-carboxylate (**11a**) (75 mg, 0.13 mmol) in dichloromethane (5.0 mL) under argon was added Grubbs second generation catalyst (0.006 g, 0.006 mmol), and the reaction mixture was stirred at room temperature overnight. The dark brown solution was concentrated under reduced pressure and the crude product was purified by column chromatography (25% ethyl acetate in hexane) to yield the title compound **12a** as a solid (0.060 g, 84%). LC–MS *t*_{R,C} = 0.523 min, [M + H]⁺ = 549.8.

tert-Butyl 2-Oxo-1-((1-tosyl-1H-indol-4-yl)methyl)-1,9-diazaspiro[5.5]undecane-9-carboxylate (13a). To a solution of *tert*-butyl 2-oxo-1-((1-tosyl-1H-indol-4-yl)methyl)-1,9-diazaspiro[5.5]undec-3-ene-9-carboxylate (**12a**) (0.12 g, 0.218 mmol) in methanol (6.0 mL) was added 10% Pd/C, and the reaction mixture was stirred

for 6 h under hydrogen (1 atm pressure) at room temperature. The reaction mixture was filtered through a pad of Celite and washed with methanol. The filtrate was concentrated, and the product **13a** was isolated as a white solid (0.120 g, 99%). LC-MS $t_{R,C} = 0.511$ min, $[M + H]^+ = 551.9$.

1-((1*H*-Indol-3-yl)methyl)-9-(quinoxalin-2-yl)-1,9-diazaspiro[5.5]undecan-2-one (14). The title compound **14** was synthesized from *tert*-butyl 4-allyl-4-((1-tosyl-1*H*-indol-3-yl)methylamino)-piperidine-1-carboxylate (**10b**) according to the procedures described for compound **16**. $^1\text{H NMR}$ (400 MHz, DMSO- d_6) δ ppm 10.79 (s, 1H), 8.78 (s, 1H), 7.80 (d, $J = 7.83$ Hz, 1H), 7.50–7.62 (m, 2H), 7.31–7.42 (m, 2H), 7.28 (d, $J = 8.07$ Hz, 1H), 7.05 (d, $J = 2.20$ Hz, 1H), 6.99 (t, $J = 8.07$ Hz, 1H), 6.79 (t, $J = 7.95$ Hz, 1H), 4.59 (s, 2H), 4.46 (d, $J = 12.47$ Hz, 2H), 3.11 (t, $J = 12.23$ Hz, 2H), 2.39 (t, $J = 6.72$ Hz, 2H), 1.97–2.20 (m, 4H), 1.69–1.85 (m, 2H), 1.61 (d, $J = 13.20$ Hz, 2H). HRMS (ESI $^+$) calcd for $\text{C}_{26}\text{H}_{28}\text{N}_5\text{O}$ (MH $^+$) 426.228 73, found 426.228 84. UPLC-MS $t_{R,A} = 1.03$ min, $[M + H]^+ = 426.3$.

1-((1*H*-Indol-4-yl)methyl)-9-(quinoxalin-2-yl)-1,9-diazaspiro[5.5]undecan-2-one (15). According to the procedures described for compound **16**, the title compound **15** was synthesized from **13a** and 2-chloroquinoxaline (45% over three steps). $^1\text{H NMR}$ (400 MHz, DMSO- d_6) δ ppm 11.05 (br s, 1H), 8.74 (s, 1H), 7.77 (d, $J = 7.83$ Hz, 1H), 7.47–7.59 (m, 2H), 7.35 (ddd, $J = 2.32, 6.05, 8.25$ Hz, 1H), 7.12–7.25 (m, 2H), 6.95 (t, $J = 7.70$ Hz, 1H), 6.64 (d, $J = 7.34$ Hz, 1H), 6.37 (br s, 1H), 4.75 (br s, 2H), 4.44 (d, $J = 12.47$ Hz, 2H), 3.10 (t, $J = 12.23$ Hz, 2H), 2.44 (t, $J = 6.72$ Hz, 2H), 2.08–2.21 (m, 2H), 1.99 (dt, $J = 4.40, 12.96$ Hz, 2H), 1.83 (td, $J = 6.24, 11.98$ Hz, 2H), 1.66 (d, $J = 12.96$ Hz, 2H). HRMS (ESI $^+$) calcd for $\text{C}_{26}\text{H}_{28}\text{N}_5\text{O}$ (MH $^+$) 426.228 84, found 426.228 96. UPLC-MS $t_{R,A} = 1.00$ min, $[M + H]^+ = 426.3$.

1-((1*H*-Indol-4-yl)methyl)-9-(4,6-dimethylpyrimidin-2-yl)-1,9-diazaspiro[5.5]undecan-2-one (16). (a) To a stirred solution of *tert*-butyl 2-oxo-1-((1-tosyl-1*H*-indol-4-yl)methyl)-1,9-diazaspiro[5.5]undecane-9-carboxylate (**13a**) (0.12 g, 0.21 mmol) in dichloromethane (5.0 mL) was added TFA (0.5 mL) at 0 °C, and the reaction mixture was stirred for 16 h at room temperature under a nitrogen atmosphere. The reaction mixture was concentrated to yield 1-((1-tosyl-1*H*-indol-4-yl)methyl)-1,9-diazaspiro[5.5]undecan-2-one trifluoroacetate as a colorless oil (0.11 g, 95%) which was used for the next step without further purification.

(b) To a stirred solution of 1-((1-tosyl-1*H*-indol-4-yl)methyl)-1,9-diazaspiro[5.5]undecan-2-one trifluoroacetate (125 mg, 0.210 mmol) in 1 mL of NMP were added 2-chloro-4,6-dimethylpyrimidine (37 mg, 0.252 mmol) and DBU (0.112 mL, 0.735 mmol), and the reaction mixture was stirred for 25 min at 110 °C in the microwave. The reaction mixture was quenched with saturated NaHCO_3 solution and extracted with TBME (2 \times 25 mL). The organic layer was washed with saturated NH_4Cl solution and brine and then dried over anhydrous Na_2SO_4 , filtered, and concentrated under reduced pressure. The crude mixture was purified by flash chromatography (3% MeOH in chloroform) to yield 9-(4,6-dimethylpyrimidin-2-yl)-1-((1-tosyl-1*H*-indol-4-yl)methyl)-1,9-diazaspiro[5.5]undecan-2-one as a white foam (67 mg, 57%). $^1\text{H NMR}$ (400 MHz, chloroform- d) δ ppm 7.82 (d, $J = 8.28$ Hz, 1 H), 7.74 (d, $J = 8.53$ Hz, 2 H), 7.54 (d, $J = 3.76$ Hz, 1 H), 7.22 (d, $J = 7.78$ Hz, 3 H), 6.89 (d, $J = 7.53$ Hz, 1 H), 6.62 (d, $J = 4.27$ Hz, 1 H), 6.26 (s, 1 H), 4.80 (br s, 2 H), 4.71 (d, $J = 18.07$ Hz, 2 H), 2.93–2.85 (m, 2 H), 2.60 (t, $J = 6.78$ Hz, 2 H), 2.35 (s, 3 H), 2.24 (s, 6 H), 2.15–2.12 (m, 2 H), 1.96–1.89 (m, 4 H), 1.63 (br s, 1 H), 1.60 (br s, 1 H), 1.53 (s, 1 H), 1.28–1.25 (m, 1 H). UPLC-MS $t_{R,A} = 1.32$ min, $[M + H]^+ = 558.4$.

(c) Cs_2CO_3 (137 mg, 0.415 mmol) was added to a stirred solution of 9-(4,6-dimethylpyrimidin-2-yl)-1-((1-tosyl-1*H*-indol-4-yl)methyl)-1,9-diazaspiro[5.5]undecan-2-one (55 mg, 0.098 mmol) in methanol (2 mL), and stirring was continued for 18 h at 78 °C. The solvent was removed under reduced pressure and the crude product was purified by flash column chromatography (ethyl acetate) to yield the title compound **16** as a white foam (37 mg, 94%). $^1\text{H NMR}$ (400 MHz, DMSO- d_6) δ ppm 7.26 (t, $J = 2.76$ Hz, 1H), 7.20 (d, $J = 8.28$ Hz, 1H), 6.96 (t, $J = 7.65$ Hz, 1H), 6.62 (d, $J = 7.03$ Hz, 1H), 6.43 (br s, 1 H), 6.32 (s, 1H), 4.72 (br s, 2H), 4.54 (d, $J = 13.80$ Hz, 2H), 2.89 (t, $J =$

12.42 Hz, 2H), 2.43 (t, $J = 6.53$ Hz, 2H), 2.14 (s, 6H), 2.09 (br s, 2H), 1.83–1.75 (m, 4H), 1.55 (d, $J = 12.80$ Hz, 2H). HRMS (ESI $^+$) calcd for $\text{C}_{24}\text{H}_{30}\text{N}_5\text{O}$ (MH $^+$) 404.244 52, found 404.244 49. UPLC-MS $t_{R,A} = 1.01$ min, $[M + H]^+ = 404.4$.

1-((1*H*-Indol-4-yl)methyl)-9-(benzo[*d*]oxazol-2-yl)-1,9-diazaspiro[5.5]undecan-2-one (17). Following the procedures described for compound **16**, the title compound **17** was synthesized from **13a** and 2-chlorobenzoxazole (52% over three steps). $^1\text{H NMR}$ (400 MHz, DMSO- d_6) δ ppm 11.06 (br s, 1H), 7.32 (d, $J = 7.83$ Hz, 1H), 7.16–7.25 (m, 3H), 7.10 (dt, $J = 0.98, 7.70$ Hz, 1H), 6.91–7.00 (m, 2H), 6.63 (d, $J = 7.09$ Hz, 1H), 6.39–6.45 (m, 1H), 4.78 (br s, 2H), 3.97 (dd, $J = 3.42, 12.96$ Hz, 2H), 3.18–3.30 (m, 2H), 2.43 (t, $J = 6.60$ Hz, 2H), 2.06–2.16 (m, 2H), 2.00 (dt, $J = 4.52, 13.02$ Hz, 2H), 1.81 (td, $J = 6.24, 11.98$ Hz, 2H), 1.63 (d, $J = 13.20$ Hz, 2H). HRMS (ESI $^+$) calcd for $\text{C}_{25}\text{H}_{27}\text{N}_4\text{O}_2$ (MH $^+$) 415.212 56, found 415.212 85. UPLC-MS $t_{R,A} = 0.97$ min, $[M + H]^+ = 415.2$.

9-(Quinoxalin-2-yl)-2,9-diazaspiro[5.5]undecan-1-one (18). To a solution of *tert*-butyl 1-oxo-2,9-diazaspiro[5.5]undecane-9-carboxylate (**8**) (2.5 g, 9.32 mmol) in dichloromethane (20 mL) was added 4 M HCl in dioxane (5 mL). The solution was stirred for 18 h at room temperature. The mixture was evaporated to dryness. The residue was crystallized from THF/heptane 3:1 to yield 2,9-diazaspiro[5.5]undecan-1-one hydrochloride as a solid (1.6 g, 82%).

To a solution of 2,9-diazaspiro[5.5]undecan-1-one hydrochloride (1.0 g, 4.89 mmol) in DMF (20 mL) were added potassium carbonate (2.03 g, 14.66 mmol) and 2-bromoquinoxaline (1.12 g, 5.37 mmol). The suspension was heated at 60 °C for 18 h. The reaction mixture was quenched with water and extracted with dichloromethane (2 \times 100 mL). The combined organic layers were dried over anhydrous Na_2SO_4 , filtered, and concentrated under reduced pressure. The crude product was purified by flash column chromatography (dichloromethane/MeOH 9:1) to yield the title compound **18** (1.13 g, 76%). $^1\text{H NMR}$ (360 MHz, DMSO- d_6) δ ppm 8.84 (s, 1H), 7.83 (d, $J = 8.08$ Hz, 1H), 7.60 (d, $J = 3.54$ Hz, 2H), 7.32–7.45 (m, 2H), 4.27 (td, $J = 4.36, 13.52$ Hz, 2H), 3.39–3.53 (m, 2H), 3.08–3.21 (m, 2H), 1.95–2.10 (m, 2H), 1.79–1.89 (m, 2H), 1.67–1.79 (m, 2H), 1.43–1.60 (m, 2H).

2-((1*H*-Indol-4-yl)methyl)-9-(quinoxalin-2-yl)-2,9-diazaspiro[5.5]undecan-1-one (19). To the suspension of 9-(quinoxalin-2-yl)-2,9-diazaspiro[5.5]undecan-1-one (**18**) (100 mg, 0.34 mmol) and NaH (17.8 mg, 0.74 mmol) in THF (5 mL) at 0 °C was added 4-(bromomethyl)-1-tosyl-1*H*-indole (147 mg, 0.41 mmol). The mixture was stirred at 50 °C for 18 h. Saturated ammonium chloride solution was added, and the mixture was extracted with dichloromethane (2 \times 50 mL). The organic layer was washed with water and brine. The combined organic layers were dried over anhydrous sodium sulfate, filtered, and evaporated to give a pale yellow oil. The crude product was purified by flash column chromatography (hexane/ethyl acetate 3:2) to yield the title compound **19** (80 mg, 55%). $^1\text{H NMR}$ (600 MHz, DMSO- d_6) δ ppm 11.14 (br s, 1H), 8.84 (s, 1H), 7.81 (d, $J = 8.28$ Hz, 1H), 7.54–7.62 (m, 2H), 7.37 (ddd, $J = 2.22, 5.95, 8.17$ Hz, 1H), 7.28–7.34 (m, 2H), 7.03 (t, $J = 7.57$ Hz, 1H), 6.82 (d, $J = 7.06$ Hz, 1H), 6.43 (br s, 1H), 4.76 (s, 2H), 4.26–4.36 (m, 2H), 3.38–3.47 (m, 2H), 3.13 (t, $J = 5.95$ Hz, 2H), 2.07–2.17 (m, 2H), 1.80–1.88 (m, 2H), 1.67–1.76 (m, 2H), 1.53–1.63 (m, 2H). HRMS (ESI $^+$) calcd for $\text{C}_{26}\text{H}_{28}\text{N}_5\text{O}$ (MH $^+$) 426.228 75, found 426.228 84. LC-MS $t_{R,B} = 2.70$ min, $[M + H]^+ = 426.4$.

***tert*-Butyl 1-Oxo-2-((1-tosyl-1*H*-indol-3-yl)methyl)-2,9-diazaspiro[5.5]undecane-9-carboxylate (20)**. To a solution of diisopropylamine (1.238 mL, 8.60 mmol) in THF (40 mL) was added *n*-butyllithium (6.01 mL, 9.61 mmol) at 0 °C, and the mixture was stirred for 30 min at 0 °C. Then a solution of *tert*-butyl 1-oxo-2,9-diazaspiro[5.5]undecane-9-carboxylate (**8**) (2.57 g, 9.28 mmol) in THF (10 mL) was added within 3 min, and the mixture was stirred for 30 min at 0 °C. 3-(Bromomethyl)-1-tosyl-1*H*-indole [S8550-81-5] (3.2 g, 8.43 mmol) in THF (10 mL) was added dropwise to the reaction mixture within 15 min. The mixture was stirred at 0 °C for 1 h and allowed to warm to room temperature overnight. The reaction mixture was quenched with ice-cold water and extracted with TBME (2 \times 150 mL). The combined organic layers were washed with 5%

aqueous citric acid and brine, dried over anhydrous Na_2SO_4 , filtered, and concentrated to yield **20** (5.3 g, 100%). ^1H NMR (400 MHz, $\text{DMSO}-d_6$) δ ppm 7.88 (d, $J = 8.28$ Hz, 1H), 7.81 (d, $J = 8.28$ Hz, 2H), 7.74 (s, 1H), 7.55 (d, $J = 7.78$ Hz, 1H), 7.36 (d, $J = 8.03$ Hz, 2H), 7.32 (t, $J = 7.91$ Hz, 1H), 7.25–7.21 (m, 1H), 4.58 (s, 2H), 3.75–3.63 (m, 2H), 3.09 (t, $J = 5.77$ Hz, 2H), 2.99 (br s, 2H), 2.30 (s, 3H), 1.90–1.80 (m, 2H), 1.72–1.57 (m, 4H), 1.39 (s, 9H), 1.36–1.28 (m, 2H). UPLC–MS $t_{\text{R,A}} = 1.37$ min, $[\text{M} + \text{H}]^+ = 552.3$.

2-((1H-Indol-3-yl)methyl)-2,9-diazaspiro[5.5]undecan-1-one (21). (a) To a solution of *tert*-butyl 1-oxo-2-((1-tosyl-1H-indol-3-yl)methyl)-2,9-diazaspiro[5.5]undecane-9-carboxylate (**20**) (5.3 g, 8.45 mmol) in dichloromethane (30 mL) was added TFA (4.93 mL, 63.4 mmol). The solution was stirred for 70 min at room temperature. The mixture was evaporated to dryness. The residue was crystallized from THF/heptane 3:1 to yield 2-((1-tosyl-1H-indol-3-yl)methyl)-2,9-diazaspiro[5.5]undecan-1-one trifluoroacetate as white crystals (5.5 g, quantitative). ^1H NMR (400 MHz, $\text{DMSO}-d_6$) δ ppm 8.43 (br s, 2H), 7.89 (d, $J = 8.28$ Hz, 1H), 7.82 (d, $J = 8.28$ Hz, 2H), 7.78 (s, 1H), 7.56 (d, $J = 7.78$ Hz, 1H), 7.38–7.31 (m, 3H), 7.24–7.20 (m, 1H), 4.59 (s, 2H), 3.29–3.19 (m, 2H), 3.12 (t, $J = 5.77$ Hz, 2H), 3.07–2.95 (m, 2H), 2.30 (s, 3H), 2.10 (ddd, $J = 14.24, 10.35, 4.02$ Hz, 2H), 1.75–1.59 (m, 4H), 1.58–1.48 (m, 2H). UPLC–MS $t_{\text{R,A}} = 0.88$ min, $[\text{M} + \text{H}]^+ = 452.3$.

(b) The suspension of 2-((1-tosyl-1H-indol-3-yl)methyl)-2,9-diazaspiro[5.5]undecan-1-one trifluoroacetate (15 g, 23.2 mmol) and C_2CO_3 (45.4 g, 139 mmol) in methanol (170 mL) was heated at reflux for 2.5 h. The solution was diluted with water and extracted with dichloromethane. The aqueous phase was adjusted to pH 11 by the addition of saturated aqueous K_2CO_3 solution, and extraction with dichloromethane was repeated. The combined organic layers were dried over sodium sulfate, filtered, and evaporated to give 6.96 g (99%) of **21** as a beige foam. ^1H NMR (400 MHz, $\text{DMSO}-d_6$) δ ppm 10.91 (br s, 1H), 7.42–7.61 (m, 1H), 7.32 (d, $J = 8.2$ Hz, 1H), 7.24 (d, $J = 2.0$ Hz, 1H), 7.04 (t, $J = 7.6$ Hz, 1H), 6.88–6.99 (m, 1H), 4.60 (s, 2H), 3.10 (t, $J = 6.1$ Hz, 2H), 2.51–2.88 (m, 4H), 1.88–2.10 (m, 3H), 1.60 (d, $J = 5.5$ Hz, 4H), 1.25–1.40 (m, 2H). LC–MS $t_{\text{R,D}} = 2.44$ min, $[\text{M} + \text{H}]^+ = 298.2$.

2-((1H-Indol-3-yl)methyl)-9-(quinoxalin-2-yl)-2,9-diazaspiro[5.5]undecan-1-one (22). The title compound was synthesized according to the procedure described for compound **26** from 2-((1H-indol-3-yl)methyl)-2,9-diazaspiro[5.5]undecan-1-one (**21**) and 2-chloroquinoxaline (60%). ^1H NMR (400 MHz, $\text{DMSO}-d_6$) δ ppm 10.92 (br s, 1H), 8.81 (s, 1H), 7.79 (d, $J = 7.82$ Hz, 1H), 7.55–7.61 (m, 2H), 7.52 (d, $J = 7.82$ Hz, 1H), 7.30–7.39 (m, 2H), 7.27 (d, $J = 1.95$ Hz, 1H), 7.05 (t, $J = 7.62$ Hz, 1H), 6.90–6.97 (m, 1H), 4.61 (s, 2H), 4.29 (td, $J = 4.40, 13.49$ Hz, 2H), 3.34–3.47 (m, 2H), 3.16 (t, $J = 5.87$ Hz, 2H), 2.03–2.16 (m, 2H), 1.74–1.84 (m, 2H), 1.60–1.72 (m, 2H), 1.45–1.57 (m, 2H). HRMS (ESI^+) calcd for $\text{C}_{26}\text{H}_{28}\text{N}_5\text{O}$ (MH^+) 426.228 88, found 426.228 84. LC–MS $t_{\text{R,B}} = 2.404$ min, $[\text{M} + \text{H}]^+ = 426.2$.

2-((1H-Indol-3-yl)methyl)-9-(pyrazin-2-yl)-2,9-diazaspiro[5.5]undecan-1-one (23). The title compound was synthesized according to the procedure described for compound **26** from 2-((1H-indol-3-yl)methyl)-2,9-diazaspiro[5.5]undecan-1-one (**21**) and 2-chloropyrazine (41%). ^1H NMR (400 MHz, $\text{DMSO}-d_6$) δ ppm 10.94 (br s, 1H), 8.30 (d, $J = 1.47$ Hz, 1H), 8.06 (dd, $J = 1.59, 2.57$ Hz, 1H), 7.78 (d, $J = 2.45$ Hz, 1H), 7.52 (d, $J = 7.82$ Hz, 1H), 7.33 (d, $J = 8.07$ Hz, 1H), 7.27 (d, $J = 2.45$ Hz, 1H), 7.05 (t, $J = 7.58$ Hz, 1H), 6.90–6.97 (m, 1H), 4.61 (s, 2H), 4.07 (td, $J = 4.22, 13.33$ Hz, 2H), 3.10–3.26 (m, 4H), 2.04 (ddd, $J = 4.40, 11.25, 13.45$ Hz, 2H), 1.72–1.81 (m, 2H), 1.60–1.71 (m, 2H), 1.39–1.51 (m, 2H). HRMS (ESI^+) calcd for $\text{C}_{22}\text{H}_{26}\text{N}_5\text{O}$ (MH^+) 376.213 39, found 376.213 19.

2-((1H-Indol-3-yl)methyl)-9-(pyrimidin-2-yl)-2,9-diazaspiro[5.5]undecan-1-one (24). The title compound was synthesized according to the procedure described for compound **26** from 2-((1H-indol-3-yl)methyl)-2,9-diazaspiro[5.5]undecan-1-one (**21**) and 2-chloropyrimidine (44%). ^1H NMR (400 MHz, $\text{DMSO}-d_6$) δ ppm 10.93 (br s, 1H), 8.34 (d, $J = 4.65$ Hz, 2H), 7.51 (d, $J = 7.82$ Hz, 1H), 7.33 (d, $J = 8.07$ Hz, 1H), 7.27 (d, $J = 2.44$ Hz, 1H), 7.05 (dt, $J = 1.10, 7.52$ Hz, 1H), 6.94 (dt, $J = 0.98, 7.46$ Hz, 1H), 6.58 (t, $J = 4.77$ Hz,

1H), 4.61 (s, 2H), 4.34 (td, $J = 4.16, 13.45$ Hz, 2H), 3.19–3.29 (m, 2H), 3.15 (t, $J = 5.99$ Hz, 2H), 1.91–2.04 (m, 2H), 1.74–1.83 (m, 2H), 1.60–1.71 (m, 2H), 1.35–1.48 (m, 2H). HRMS (ESI^+) calcd for $\text{C}_{22}\text{H}_{26}\text{N}_5\text{O}$ (MH^+) 376.213 17, found 376.213 19.

2-((1H-Indol-3-yl)methyl)-9-(4-methylpyrimidin-2-yl)-2,9-diazaspiro[5.5]undecan-1-one (25). The title compound was synthesized according to the procedure described for compound **26** from 2-((1H-indol-3-yl)methyl)-2,9-diazaspiro[5.5]undecan-1-one (**21**) and 2-chloro-4-methylpyrimidine (74%). ^1H NMR (400 MHz, $\text{DMSO}-d_6$) δ ppm 8.19 d, $J = 4.77$ Hz, 1H), 7.52 (d, $J = 7.78$ Hz, 1H), 7.33 (d, $J = 8.03$ Hz, 1H), 7.27 (d, $J = 2.26$ Hz, 1H), 7.05 (t, $J = 7.53$ Hz, 1H), 6.96–6.92 (m, 1H), 6.47 (d, $J = 4.77$ Hz, 1H), 4.61 (s, 2H), 4.40–4.31 (m, 2H), 3.26–3.11 (m, 4H), 2.26 (s, 3H), 2.02–1.91 (m, 2H), 1.82–1.74 (m, 2H), 1.70–1.61 (m, 2H), 1.45–1.37 (m, 2H). HRMS (ESI^+) calcd for $\text{C}_{23}\text{H}_{28}\text{N}_5\text{O}$ (MH^+) 390.228 85, found 390.228 84. UPLC–MS $t_{\text{R,A}} = 1.04$ min, $[\text{M} + \text{H}]^+ = 390.2$.

2-((1H-Indol-3-yl)methyl)-9-(4-methoxypyrimidin-2-yl)-2,9-diazaspiro[5.5]undecan-1-one (26). To the solution of 2-((1H-indol-3-yl)methyl)-2,9-diazaspiro[5.5]undecan-1-one (**21**) (3.4 g, 11.32 mmol) in acetonitrile (10 mL) in a microwave tube were added 2-chloro-4-methoxypyrimidine (2.17 g, 14.71 mmol), DIPEA (6.99 mL, 39.6 mmol), and DBU (0.052 mL, 0.34 mmol). The tube was sealed, and the reaction mixture was heated at 120 °C for 2 h under microwave conditions. The solvent was removed under reduced pressure. The resulting crude product was purified by flash chromatography (heptane/EtOAc 55/45 to heptane/EtOAc 13/87). The product was crystallized from TBME to give the title compound **26** as white crystals (3.33 g, 72%). ^1H NMR (400 MHz, $\text{DMSO}-d_6$) δ ppm 8.07 (d, $J = 5.52$ Hz, 1H), 7.52 (d, $J = 7.78$ Hz, 1H), 7.33 (d, $J = 8.28$ Hz, 1H), 7.27 (d, $J = 2.26$ Hz, 1H), 7.05 (t, $J = 7.65$ Hz, 1H), 6.96–6.92 (m, 1H), 6.03 (d, $J = 5.52$ Hz, 1H), 4.62 (s, 2H), 4.34 (ddd, $J = 13.43, 4.14, 4.02$ Hz, 2H), 3.82 (s, 3H), 3.28–3.19 (m, 2H), 3.15 (t, $J = 6.02$ Hz, 2H), 2.04–1.93 (m, 2H), 1.81–1.74 (m, 2H), 1.70–1.61 (m, 2H), 1.47–1.38 (m, 2H). HRMS (ESI^+) calcd for $\text{C}_{23}\text{H}_{28}\text{N}_5\text{O}_2$ (MH^+) 406.223 75, found 406.223 43. UPLC–MS $t_{\text{R,A}} = 0.96$ min, $[\text{M} + \text{H}]^+ = 406.4$.

2-((1H-Indol-3-yl)methyl)-9-(4,6-dimethylpyrimidin-2-yl)-2,9-diazaspiro[5.5]undecan-1-one (27). The title compound was synthesized according to the procedure described for compound **26** from 2-((1H-indol-3-yl)methyl)-2,9-diazaspiro[5.5]undecan-1-one (**21**) and 2-chloro-4,6-dimethylpyrimidine (56%). ^1H NMR (400 MHz, $\text{DMSO}-d_6$) δ ppm 7.52 (d, $J = 8.03$ Hz, 1H), 7.27 (d, $J = 2.01$ Hz, 1H), 7.05 (t, $J = 7.53$ Hz, 1H), 6.96–6.92 (m, 1H), 6.36 (s, 1H), 4.61 (s, 2H), 4.42–4.33 (m, 2H), 3.23–3.09 (m, 4H), 2.21 (s, 6H), 2.01–1.90 (m, 2H), 1.81–1.73 (m, 2H), 1.70–1.60 (m, 2H), 1.45–1.33 (m, 2H). HRMS (ESI^+) calcd for $\text{C}_{24}\text{H}_{30}\text{N}_5\text{O}$ (MH^+) 404.244 49, found 404.244 76. UPLC–MS $t_{\text{R,A}} = 1.11$ min, $[\text{M} + \text{H}]^+ = 404.4$.

9-(4,6-Dimethylpyrimidin-2-yl)-2-((1-methyl-1H-indol-3-yl)methyl)-2,9-diazaspiro[5.5]undecan-1-one (28). NaH (10 mg, 0.26 mmol, 60% in mineral oil) was added to an ice-cold solution of 2-((1H-indol-3-yl)methyl)-9-(4,6-dimethylpyrimidin-2-yl)-2,9-diazaspiro[5.5]undecan-1-one (**27**) (69 mg, 0.17 mmol) in THF (3 mL). The resulting mixture was stirred at 0 °C for 10 min. Then methyl iodide (0.02 mL, 0.26 mmol) was added at 0 °C and the reaction mixture was allowed to warm to room temperature over a period of 18 h. The mixture was poured into water and the solution was extracted twice with ethyl acetate. The combined organic layers were washed with water and brine, filtered, and dried over anhydrous sodium sulfate. The organic layer was concentrated under reduced pressure. The product was purified by preparative HPLC (column AG/PP-C18-15/021, flow 20 mL/min, mobile phase 0.1% TFA in water (A), acetonitrile (B) gradient) to yield the title compound **28** (18 mg, 25%). ^1H NMR (400 MHz, $\text{DMSO}-d_6$) δ ppm 7.53 (d, $J = 8.07$ Hz, 1H), 7.37 (d, $J = 8.31$ Hz, 1H), 7.25 (s, 1H), 7.12 (t, $J = 8.19$ Hz, 1H), 6.93–7.03 (m, 1H), 6.36 (s, 1H), 4.59 (s, 2H), 4.37 (td, $J = 3.97, 13.33$ Hz, 2H), 3.73 (s, 3H), 3.09–3.24 (m, 4H), 2.21 (s, 6H), 1.89–2.01 (m, 2H), 1.72–1.82 (m, 2H), 1.59–1.71 (m, 2H), 1.33–1.45 (m, 2H). HRMS (ESI^+) calcd for $\text{C}_{25}\text{H}_{32}\text{N}_5\text{O}$ (MH^+) 418.260 36, found 418.260 14. UPLC–MS $t_{\text{R,A}} = 1.27$ min, $[\text{M} + \text{H}]^+ = 418.3$.

9-(4,6-Dimethylpyrimidin-2-yl)-2,9-diazaspiro[5.5]undecan-1-one (29). (a) To a solution of *tert*-butyl 1-oxo-2,9-diazaspiro[5.5]undecane-9-carboxylate (**8**) (20.0 g, 72.3 mmol) in dichloromethane (200 mL) was added TFA (56.3 mL, 723 mmol) at 0 °C. The solution was allowed to warm to room temperature and stirred for 1 h. The mixture was evaporated to dryness. The residue was dried under high vacuum to yield 2,9-diazaspiro[5.5]undecan-1-one trifluoroacetate as a solid (41.9 g, quantitative). ¹H NMR (400 MHz, DMSO-*d*₆) δ ppm 8.41 (br s, 2H), 7.46 (br s, 1H), 3.18–3.32 (m, 2H), 2.95–3.14 (m, 4H), 1.98–2.10 (m, 2H), 1.61–1.75 (m, 4H), 1.46–1.58 (m, 2H). UPLC–MS *t*_{R,A} = 0.21 min, [M + H]⁺ = 169.2

(b) To a solution of 2,9-diazaspiro[5.5]undecan-1-one trifluoroacetate (1.4 g, 4.96 mmol) in ethanol (11 mL) in a microwave tube were added 2-chloro-4,6-dimethylpyrimidine (0.875 g, 6.0 mmol), DIPEA (4.3 mL, 25 mmol), and DMAP (30 mg, 0.25 mmol). The tube was sealed, and the suspension was heated at 160 °C for 2 h under microwave conditions. The solvent was removed under reduced pressure. The resulting crude product was taken up in ethanol and filtered and the solid washed with ethanol. The filtrate was concentrated. The precipitate from the filtrate was filtered and washed with ethanol, and the combined solids were taken up in ethyl acetate. The ethyl acetate layer was washed with water and brine and dried over anhydrous sodium sulfate. The organic layer was filtered and concentrated under reduced pressure to give 1.02 g (75%) of **29** as a white solid. ¹H NMR (600 MHz, DMSO-*d*₆) δ ppm 7.34 (br s, 1H), 6.36 (s, 1H), 4.19–4.38 (m, 2H), 3.23 (t, *J* = 11.10 Hz, 2H), 3.03–3.15 (m, 2H), 2.21 (s, 6H), 1.81–1.92 (m, 2H), 1.75–1.81 (m, 2H), 1.63–1.73 (m, 2H), 1.40 (d, *J* = 13.32 Hz, 2H). UPLC–MS *t*_{R,A} = 0.69 min, [M + H]⁺ = 275.3.

9-(4,6-Dimethylpyrimidin-2-yl)-2-((5-methoxy-1*H*-indol-3-yl)methyl)-2,9-diazaspiro[5.5]undecan-1-one (30). The title compound was synthesized according to the procedure described for compound **32** starting from 9-(4,6-dimethylpyrimidin-2-yl)-2,9-diazaspiro[5.5]undecan-1-one (**29**) and 3-(bromomethyl)-5-methoxy-1-tosyl-1*H*-indole⁵⁹ (88% over two steps). ¹H NMR (400 MHz, DMSO-*d*₆) δ ppm 10.80 (s, 1H), 7.20–7.28 (m, 2H), 7.06 (d, *J* = 2.38 Hz, 1H), 6.71 (dd, *J* = 2.45, 8.72 Hz, 1H), 6.38 (s, 1H), 4.60 (s, 2H), 4.39 (td, *J* = 3.89, 13.30 Hz, 2H), 3.69 (s, 3H), 3.08–3.25 (m, 4H), 2.23 (s, 6H), 1.93–2.05 (m, 2H), 1.74–1.83 (m, 2H), 1.61–1.72 (m, 2H), 1.37–1.48 (m, 2H). HRMS (ESI⁺) calcd for C₂₅H₃₂N₅O₂ (MH⁺) 434.255 05, found 434.255 35. UPLC–MS *t*_{R,A} = 1.06 min, [M + H]⁺ = 434.3.

2-((1*H*-Indazol-3-yl)methyl)-9-(4,6-dimethylpyrimidin-2-yl)-2,9-diazaspiro[5.5]undecan-1-one (31). The title compound was synthesized according to the procedure described for compound **32** starting from 9-(4,6-dimethylpyrimidin-2-yl)-2,9-diazaspiro[5.5]undecan-1-one (**29**) and 3-(bromomethyl)-1-tosyl-1*H*-indazole⁵⁹ (75% over two steps). ¹H NMR (400 MHz, DMSO-*d*₆) δ ppm 12.86 (s, 1H), 7.67 (d, *J* = 8.03 Hz, 1H), 7.47 (d, *J* = 8.53 Hz, 1H), 7.32 (t, *J* = 7.53 Hz, 1H), 7.06 (t, *J* = 7.40 Hz, 1H), 6.36 (s, 1H), 4.81 (s, 2H), 4.37 (td, *J* = 3.98, 13.36 Hz, 2H), 3.11–3.25 (m, 4H), 2.21 (s, 6H), 1.88–2.02 (m, 2H), 1.74–1.85 (m, 2H), 1.61–1.73 (m, 2H), 1.35–1.48 (m, 2H). HRMS (ESI⁺) calcd for C₂₃H₂₉N₆O (MH⁺) 405.239 74, found 405.239 98. UPLC–MS *t*_{R,A} = 0.99 min, [M + H]⁺ = 405.3.

2-((1*H*-Pyrrolo[2,3-*b*]pyridin-3-yl)methyl)-9-(4,6-dimethylpyrimidin-2-yl)-2,9-diazaspiro[5.5]undecan-1-one (32). To the suspension of 9-(4,6-dimethylpyrimidin-2-yl)-2,9-diazaspiro[5.5]undecan-1-one (**29**) (100 mg, 0.36 mmol) and TBAI (13 mg, 0.04 mmol) in anhydrous THF (4 mL) at 0 °C was added NaH (95%, 18 mg, 0.73 mmol). After the mixture was stirred for 20 min, 3-(bromomethyl)-1-tosyl-1*H*-pyrrolo[2,3-*b*]pyridine⁵⁹ (172 mg, 0.40 mmol) was added and stirring was continued at room temperature for 2.5 h. Water was added, and the aqueous layer was extracted with ethyl acetate. The organic layer was washed with water and brine. The combined organic layers were dried over anhydrous sodium sulfate, filtered, and evaporated to give a pale yellow oil. The crude product was purified by flash column chromatography (hexane/ethyl acetate 3:2) to yield a white solid (188 mg, 92%). LC–MS *t*_{R,D} = 2.59 min, [M + H]⁺ = 559.2.

The white solid (188 mg) was then dissolved in MeOH (3 mL), and Cs₂CO₃ (439 mg, 1.35 mmol) was added. The mixture was stirred at 70 °C for 90 min and then cooled to room temperature. Brine was added and the aqueous phase extracted with EtOAc. Then the combined organic phases were washed with brine, dried over Na₂SO₄, filtered and the solvent was removed under reduced pressure to give a pale yellow residue. Crystallization from a minimum of hot Et₂O/TBME yielded **32** as a pale yellow solid (100 mg, 73%). ¹H NMR (400 MHz, DMSO-*d*₆) δ ppm 11.47 (br s, 1H), 8.17 (d, *J* = 4.30 Hz, 1H), 7.90 (d, *J* = 7.43 Hz, 1H), 7.40 (d, *J* = 2.35 Hz, 1H), 7.01 (dd, *J* = 8.02, 4.50 Hz, 1H), 6.35 (s, 1H), 4.58 (s, 2H), 4.31–4.42 (m, 2H), 3.12–3.22 (m, 4H), 2.21 (s, 6H), 1.88–2.00 (m, 2H), 1.73–1.81 (m, 2H), 1.66 (d, *J* = 5.87 Hz, 2H), 1.39 (d, *J* = 13.69 Hz, 2H). HRMS (ESI⁺) calcd for C₂₃H₂₉N₆O (MH⁺) 405.239 74, found 405.239 61. LC–MS *t*_{R,D} = 2.34 min, [M + H]⁺ = 405.2.

9-(4,6-Dimethylpyrimidin-2-yl)-2-((4-phenyl-1*H*-pyrazol-3-yl)methyl)-2,9-diazaspiro[5.5]undecan-1-one (34). The title compound was synthesized according to the procedure described for compound **35** starting from 9-(4,6-dimethylpyrimidin-2-yl)-2,9-diazaspiro[5.5]undecan-1-one (**29**) and 3-(bromomethyl)-4-phenyl-1-((2-(trimethylsilyl)ethoxy)methyl)-1*H*-pyrazole (**33a**)⁵⁹ (91% over two steps). ¹H NMR (600 MHz, DMSO-*d*₆) δ ppm 12.82 (br s, 1H), 7.64–7.99 (m, 1H), 7.26–7.39 (m, 4H), 7.16–7.24 (m, 1H), 6.34 (s, 1H), 4.67 (br s, 2H), 4.16–4.30 (m, 2H), 3.14–3.26 (m, 2H), 3.00–3.13 (m, 2H), 2.19 (s, 6H), 1.75–1.87 (m, 2H), 1.54–1.75 (m, 4H), 1.24–1.33 (m, 2H). HRMS (ESI⁺) calcd for C₂₅H₃₁N₆O (MH⁺) 431.255 39, found 431.255 31. LC–MS *t*_{R,D} = 2.804 min, [M + H]⁺ = 431.2.

9-(4,6-Dimethylpyrimidin-2-yl)-2-((5-phenyl-2*H*-1,2,3-triazol-4-yl)methyl)-2,9-diazaspiro[5.5]undecan-1-one (35). To a suspension of 9-(4,6-dimethylpyrimidin-2-yl)-2,9-diazaspiro[5.5]undecan-1-one (**29**) (150 mg, 0.541 mmol) and TBAI (20.2 mg, 0.054 mmol) in dry THF (5 mL) at 0 °C under argon was added NaH (60%, 44 mg, 1.08 mmol). After the mixture was stirred for 20 min, a solution of 4-(bromomethyl)-5-phenyl-2-((2-(trimethylsilyl)ethoxy)methyl)-2*H*-1,2,3-triazole (**33b**)⁵⁹ (222 mg, 0.595 mmol) in dry THF (0.5 mL) was added. The mixture was allowed to cool to room temperature and stirred for 4 h. Water was added, and the reaction mixture was extracted with dichloromethane. The organic layer was washed with water and brine and dried over anhydrous sodium sulfate, filtered, and concentrated under reduced pressure. The resulting crude product was used without further purification in the next step (400 mg, 99%). UPLC–MS *t*_{R,A} = 1.56 min, [M + H]⁺ = 562.5.

The residue (395 mg, 0.527 mmol) was dissolved in EtOH (3 mL), and aqueous 6 M HCl (3.0 mL, 18.0 mmol) was added. The reaction mixture was stirred at 90 °C for 1 h. The reaction mixture was allowed to warm to room temperature. Saturated aqueous NaHCO₃ solution was added and the mixture was extracted with TBME (2×). The combined organic phases were washed with water and brine, dried over anhydrous sodium sulfate, filtered, and evaporated to give a pale yellow oil. The crude product was purified by flash chromatography (10% EtOAc in heptane to 100% EtOAc). The product was crystallized from diisopropyl ether to give the title compound **35** as white crystals (76 mg, 32% over two steps). ¹H NMR (400 MHz, DMSO-*d*₆) δ ppm 7.64 (d, *J* = 7.28 Hz, 2H), 7.31–7.50 (m, 3H), 6.35 (s, 1H), 4.77 (s, 2H), 4.15–4.37 (m, 2H), 3.11–3.26 (m, 4H), 2.20 (s, 6H), 1.79–1.92 (m, 2H), 1.61–1.78 (m, 4H), 1.26–1.42 (m, 2H). HRMS (ESI⁺) calcd for C₂₄H₃₀N₇O (MH⁺) 432.250 63, found 432.250 84. UPLC–MS *t*_{R,A} = 0.98 min, [M + H]⁺ = 432.4.

9-(4,6-Dimethylpyrimidin-2-yl)-2-((1-methyl-4-phenyl-1*H*-pyrazol-3-yl)methyl)-2,9-diazaspiro[5.5]undecan-1-one (36). The title compound was synthesized according to the procedure described for compound **37** starting from 9-(4,6-dimethylpyrimidin-2-yl)-2-((4-phenyl-1*H*-pyrazol-3-yl)methyl)-2,9-diazaspiro[5.5]undecan-1-one (**34**) (74% yield). ¹H NMR (600 MHz, DMSO-*d*₆) δ ppm 7.92 (s, 1H), 7.28–7.37 (m, 4H), 7.18–7.26 (m, 1H), 6.36 (s, 1H), 4.65 (s, 2H), 4.19–4.32 (m, 2H), 3.82 (s, 3H), 3.20 (t, *J* = 12.82 Hz, 2H), 3.09 (t, *J* = 5.65 Hz, 2H), 2.21 (s, 6H), 1.75–1.85 (m, 2H), 1.56–1.71 (m, 4H), 1.24–1.31 (m, 2H). HRMS (ESI⁺) calcd for C₂₆H₃₃N₆O (MH⁺)

445.271 04, found 445.270 74. LC–MS $t_{R,D}$ = 2.903 min, $[M + H]^+$ = 445.2.

9-(4,6-Dimethylpyrimidin-2-yl)-2-((2-methyl-5-phenyl-2H-1,2,3-triazol-4-yl)methyl)-2,9-diazaspiro[5.5]undecan-1-one (37). To a solution of 9-(4,6-dimethylpyrimidin-2-yl)-2-((5-phenyl-2H-1,2,3-triazol-4-yl)methyl)-2,9-diazaspiro[5.5]undecan-1-one (35, 250 mg, 0.556 mmol) and methyl iodide (0.078 mL, 0.834 mmol) in dry THF (4 mL) at 0 °C under argon was added NaH (60%, 28 mg, 0.695 mmol). After 90 min at 0 °C the reaction mixture was allowed to warm to room temperature and stirred for 4 h. Saturated aqueous NaHCO₃ solution was added, and the mixture was extracted with TBME (2×). The combined organic layers were washed with water and brine, dried over anhydrous sodium sulfate, filtered, and evaporated to give a pale yellow residue. The crude product was purified by flash chromatography (10% EtOAc in heptane to 100% EtOAc) to yield the title compound and a regioisomer. The product was crystallized from diisopropyl ether to give the title compound 37 as white crystals (74 mg, 30%). ¹H NMR (400 MHz, DMSO-*d*₆) δ ppm 7.61 (dd, *J* = 1.25, 8.03 Hz, 2H), 7.33–7.46 (m, 3H), 6.34 (s, 1H), 4.74 (s, 2H), 4.27 (td, *J* = 4.14, 13.30 Hz, 2H), 4.14 (s, 3H), 3.12–3.26 (m, 4H), 2.20 (s, 6H), 1.77–1.89 (m, 2H), 1.61–1.76 (m, 4H), 1.27–1.39 (m, 2H). HRMS (ESI⁺) calcd for C₂₅H₃₂N₇O (MH⁺) 446.266 46, found 446.266 28. UPLC–MS $t_{R,A}$ = 1.19 min, $[M + H]^+$ = 446.3.

B. Biology. All animals were maintained under standard housing conditions with access to standard pelleted food and water ad libitum, including throughout experiments. The animal experiments were conducted in accordance with Swiss national animal welfare regulations, under the ethically approved animal experimentation licenses authorized by the Cantonal Veterinary Authority of Basel City and the Federal Veterinary Office of Switzerland.

Calcium Accumulation in Cells (FLIPR). Chinese hamster ovary cells and human embryo kidney cells expressing human and mouse OX₁R or OX₂R receptors respectively, grown in Dulbecco's minimum essential medium (DMEM)/F12/10% fetal calf serum (FCS) were seeded at 8000 cells/well in 384 well black-walled clear bottom, poly-D-lysine coated plates. After 24 h, the medium was removed and cells were washed once with phosphate buffered saline and serum-deprived overnight in assay buffer (130 mM NaCl, 5.4 mM KCl, 1.8 mM CaCl₂, 0.8 mM MgSO₄, 0.9 mM NaH₂PO₄, 25 mM glucose, 20 mM HEPES, pH 7.4) containing bovine serum albumin (1% w/v).

On the day of the experiment, the cells seeded in black plates were treated with assay buffer containing the Ca²⁺ sensitive fluorescent dye Fluo4-AM (2 μ M) and probenecid (0.1 mM). After 1 h, plates were washed twice with, and resuspended in, assay buffer containing probenecid (0.1 mM) using a multiplate washer. The plates were placed into a FLIPR II (fluorometric imaging plate reader, FLIPR-384, Molecular Devices, Sunnyvale, CA, USA), and baseline fluorescence (fluorescence light units, FLU) was measured (five measurements, 2 s each, laser excitation 488 nm at 0.6–1 W, CCD camera exposure 0.4 s) before addition of buffer alone (basal) or containing test compounds (either test compound alone, agonist alone, or agonist in the presence of various concentrations of a test compound). Fluorescence measurements were then continued every 1 s for 120 s followed by every 4 s for 240 s.

The measurements were typically made in two sequences: In the first round, compounds were tested alone to confirm that they do not display any significant agonist activity. Compounds were tested usually in a concentration range from 10⁻⁹ to 10⁻⁵ M. In the second round, performed 1 h later (to allow for equilibration), orexin A was tested either in the absence (calibration curves, orexin A agonist controls) or in the presence of test compounds to determine antagonism.

Inhibition data is expressed as pK_i [$-\log M$], converted by the Cheng and Prusoff correction ($K_i = IC_{50}/[1 + (L/EC_{50})]$), where IC₅₀ is the 50% inhibition value determined in concentration–response inhibition curves, EC₅₀ is the half maximal activation concentration determined for orexin A in concentration–response curves, and *L* is the concentration of orexin A used in inhibition experiments performed with a submaximal concentration of orexin A in the

presence of up to eight increasing concentrations of test compounds. All concentration–response curves were run in triplicate.

Mouse PK Experiments. Pharmacokinetic Study. A cassette dosing approach (up to five compounds and one reference from the same chemical series) was chosen in order to obtain pharmacokinetic parameter and information about the brain penetration properties of a series of chemically similar compounds in a timely fashion with a higher throughput. A reference compound with known PK properties was always included to validate the cassette dosing. For iv injection, 1 mg/kg of each test compound was individually solubilized in *N*-methylpyrrolidone, then mixed together and finally diluted in blank plasma. The final formulation mixture (NMP/blank plasma 10/90, v/v) was administered at 5 mL/kg body weight into the saphenous vein of male C57BL/6 mice, weighing between 20 and 30 g (from Iffa-Credo, France). Blood was collected by sublingual bleeding (~70 μ L/mouse) or at sacrifice (~300 μ L/mouse) at 5 and 30 min and 1, 2, 4, 6, 8, and 24 h pd. The brain was collected after decapitation at 5 min and at 1, 4, and 24 h pd. For oral dosing, 3 mg/kg of each test compound was individually suspended in carboxymethylcellulose 0.5% w/v in water/Tween 80 (99.5%/0.5%, v/v). Suspensions were mixed together and applied by oral gavage to mice to deliver a final dose volume of 10 mL/kg body weight. The blood and brain samples were collected at the same time points as after intravenous administration with the exception that the first blood and brain samples were collected after 15 min pd.

Similarly, mice in the satellite PK group for the in vivo efficacy studies received 50 mg/kg test compound suspended in methylcellulose 0.5% w/v in water by oral gavage at a dose volume of 10 mL/kg body weight. Blood and brain samples were collected after decapitation at 15 and 60 min after dosing. All PK experiments were run with *n* = 3 mice per sampling time point. The blood and brain samples were stored at –20 °C until analysis by LC/MS/MS.

Bioanalytical Method. The brain samples were homogenized with 2 mM KH₂PO₄ buffer (approximately 1/2, w/v). A structurally similar internal standard was added to the blood or brain homogenate samples, and the test compounds were extracted by quenching with a 4-fold volume of acetonitrile. After centrifugation an aliquot of the supernatant was directly injected into the LC/MS/MS system (CTC PAL autosampler, Rheos Allegro LC pump, TSQ Quantum MS, all from Thermo Scientific, Waltham, MA, U.S.). The specific analytical conditions, i.e., type of the LC column, mobile phase, ionization mode, ion source parameter, and MRM transitions, were adapted to the respective cassette dosing experiment to achieve optimal chromatographic separation and sensitive detection of the test compounds. Quantitative drug concentrations were obtained based on a six-level calibration curve, using quadratic fitting of a weighed plot of the log–log transformed peak area ratios vs the blood concentrations. Usually, the LLOQ ranged between 0.4 and 2 ng/mL in blood and between 1.2 and 6 ng/g in brain.

PK Data Analysis. The absorption and disposition parameters were estimated by a noncompartmental analysis of the mean blood concentration (*n*=3) versus time profile after oral and intravenous administration. The apparent terminal phase rate constant was determined by choosing the last three data points from the log–linear regression of the blood concentrations versus time curve and was used for the extrapolation of the AUC to infinity. The absolute oral bioavailability was calculated by dividing the dose-normalized AUC after oral administration by the respective AUC after intravenous administration assuming linear pharmacokinetics between the doses of 3 and 1 mg/kg, respectively.

Locomotor Paradigm in Mouse. For measuring the effects of compounds on locomotor activity, a computerized motility measurement system was used (Moti 4.25, TSE Systems, Bad Homburg, Germany). This system automatically measures locomotor activity in transparent boxes (20 cm × 32 cm × 17 cm) by counting the interruptions of horizontal infrared beams spaced 5.7–8.4 cm apart in a frame set at the floor level of the cage.

C57Bl/6 mice (Janvier, Le Genest Saint Isle, France) adapted to a 12h/12h light/dark cycle with lights off at 15:00 were individually placed into these cages at about 9:00 and were allowed to habituate for

1.5 days. Immediately before lights-off (15:00) on the following day, animals were treated with either vehicle control (0.5% methylcellulose in water, w/v), **26** (in MEPC5 40%), or suvorexant (0.5% methylcellulose in water, w/v). Fifteen hours later, the animals were brought back to their home cages.

One minute of inactivity was defined as a minute without any interruptions of the infrared beams. Previous studies demonstrated that this measure is highly correlated with sleep.⁵³ To analyze compounds effects, the difference in inactivity in the 4 h after compound administration (15:00 to 19:00) and the inactivity during the same 4 h at 24 h earlier (during the habituation phase) were calculated for each animal. Treatment group mean values were then compared using an analysis of variance (one-way ANOVA) with post hoc Dunnett's tests (comparisons with vehicle).

Mouse Sleep Assay. *Implantation of Electroencephalogram/Electroencephalogram (EEG) and Electromyogram (EMG) Electrodes.* Male C57Bl/6 mice were administered temgesic (0.05 mg/kg sc) 1 h before surgery. Mice were anesthetized with ketamine/xylazine (110 mg/kg, 10:1, ip) and placed in a stereotaxic frame. The skull was exposed, and four miniature stainless steel screws (SS-5/TA Science Products GmbH, Hofheim Germany) attached to 36-gauge Teflon coated solid silver wires were placed in contact with the frontal and parietal cortex (3 mm posterior to bregma, ± 2 mm from the sagittal suture) through bore holes. The frontal electrodes served as reference. The wires were crimped to a small six-channel connector (CRISTEK Micro Strip Connector) that was affixed to the skull with dental acrylic. EMG signals were acquired by a pair of multistranded stainless steel wires (7SS-1T, Science Products GmbH, Hofheim, Germany) inserted into the neck muscles and also crimped to the headmount. After surgery, mice were singly housed and allowed to recover in their cage placed on a heating pad. Temgesic, 0.05 mg/kg, sc, was given 8 and 16 h after surgery to prevent pain. After 24 h, the mice were housed with their former cage mates and allowed to recover for 2 weeks. Mice were continuously kept on a 12 h/12 h light/dark cycle with lights on at 03:00.

Sleep Studies. Mice were habituated to individual cages in the sound-attenuated recording chamber for 6–10 days (lights on 03:00, lights off 15:00, max 80 lx) and a constant temperature of about 23 °C. Mice had access to food and water ad libitum and access to one nesting paper and a piece of wood. Mice were weighed and attached to recording cables that connected their head mounts to a commutator (G-4-E, Gaueschi) allowing free movement in the experiment boxes on the morning of the first day of the experiment. All further manipulations and oral applications were performed in a time window of 5–15 min before lights off and start of the recordings. On day 1, the mice were manipulated and habituated to the oral application syringe just before lights off. On day 2, they received vehicle (methylcellulose 0.5%, 10 mL/kg, per os). On day 3, **26** or suvorexant was administered per os. Recordings began with lights off at 15:00 (hour 0) and continued for 23 h. The experimental chamber was secured about 5 min prior to lights off, and the mice were undisturbed during the recordings. One hour before lights off, recordings were stopped and the chamber was opened to care for the mice and perform any manipulations necessary. On day 4, the mice were replaced in groups in their normal housing cages. EEG/EMG signals were amplified using a Grass model 78D amplifier (Grass Instrument CO., Quincy, MA, USA), analogue filtered (EEG, 0.3–30 Hz; EMG, 5–30 Hz) and acquired using Harmonie V5.2 (acquisition frequency of 200 Hz with calibration the first day, record duration of 23 h). Animals were videorecorded during data collection, using an infrared video camera, and locomotor activity was detected using infrared sensors (InfraMot infrared activity sensor 30-2015 SENS, TSE Systems) placed in the roof of the boxes. Activity signals were acquired at 10 s intervals by the software Labmaster V2.4.4. EEG/EMG and activity recordings were imported into and scored in 10 s epochs using the rodent scoring module of Somnologica into wake, NREM sleep, and REM sleep. Epochs during which there were state transitions were scored as the state present for at least 50% of the epoch. The time in each state per hour was calculated, and the mean \pm SEM is shown. Restricted maximum likelihood analysis (REML) was applied to determine if

there was a statistically significant effect of treatment or a significant interaction between treatment and hour. Post hoc Fisher's least significant difference tests were applied to determine hour by hour where there were significant differences between the vehicle and compound days.

AUTHOR INFORMATION

Corresponding Authors

*C.B.: phone, +41 61 6967739; e-mail, claudia.betschart@novartis.com. For

*S.H.: phone, +41 61 6968456; e-mail, samuel.hintermann@novartis.com.

Present Addresses

¹D.H.: Department of Pharmacology & Therapeutics, Faculty of Medicine, Dentistry and Health Sciences, School of Medicine, The University of Melbourne, Parkville, Victoria 3010, Australia. E-mail: d.hoyer@unimelb.edu.au

[#]C.E.G.: Institute for Synaptic Physiology, Center for Molecular Neurobiology Hamburg, Falkenried 94, 20251 Hamburg, Germany. E-mail: christine.gee@zmn.uni-hamburg.de.

[∞]M.F.: Institute for Pharmacology and Toxicology, Otto-von-Guericke University Magdeburg, Leipziger Strasse 44, D-39120 Magdeburg, Germany. E-mail: markus.fendt@med.ovgu.de.

[×]V.C.: Department of Medicinal Chemistry, Lupin Pharmaceuticals, Inc., Lupin Research Park, Genesis Square, Phase-II, Hinjewadi, Pune-411057, India. E-mail: vinodchaudhari@lupinpharma.com.

●L.H.J.: The Florey Institute of Neuroscience and Mental Health, The University of Melbourne, Kenneth Myer Building, Genetics Lane on Royal Parade, Victoria 3010, Australia. E-mail: ljacobson@unimelb.edu.au.

Author Contributions

○C.B. and S.H. contributed equally.

The manuscript was written through contributions of all authors. All authors have given approval to the final version of the manuscript.

Notes

The authors declare no competing financial interest.

ACKNOWLEDGMENTS

We thank Richard Felber, Sandrine Liverneaux, Andrea Hasler, Alfred Tanner, Thomas Gut, Marc Weibel, Fatma Limam, Marjorie Bourrel, and Michael Wright for synthetic support, Christian Guenat for the determination of high resolution mass, Thomas Dürst, Stefan Imobersteg, Hugo Bürki, Edi Schuepbach, Daniel Langenegger, and Dominique Monna for in vitro and in vivo studies, Agnese Vit and Karen Beltz for compound formulation support, and Eric Legangneux for helpful discussions.

ABBREVIATIONS USED

AUC_{bl}, area under the blood concentration time curve; [bl], blood concentration; [br] brain concentration; Cl_{bl}, total blood clearance; C_{max}, observed maximum concentration in blood; DORA, dual orexin receptor antagonist; EMG, electromyogram; f_w, free fraction; FLIPR, fluorometric imaging plate reader; LC/MS/MS, liquid chromatography coupled to tandem mass spectrometry; LipE, lipophilicity efficiency; LLOQ, lower limit of quantification; NREM, nonrapid eye movement sleep; OX₁R, orexin (hypocretin) receptor type 1; OX₂R, orexin (hypocretin) receptor type 2; OXR, orexin receptor; pd,

postdosing; REM, rapid eye movement sleep; V_{ss} , apparent volume of distribution at steady state

REFERENCES

- (1) Sakurai, T.; Amemiya, A.; Ishii, M.; Matsuzaki, I.; Chemelli, R. M.; Tanaka, H.; Williams, S. C.; Richardson, J. A.; Kozlowski, G. P.; Wilson, S.; Arch, J. R. S.; Buckingham, R. E.; Haynes, A. C.; Carr, S. A.; Annan, R. S.; McNulty, D. E.; Liu, W.-S.; Terrett, J. A.; Elshourbagy, N. A.; Bergsma, D. J.; Yanagisawa, M. Orexins and orexin receptors: a family of hypothalamic neuropeptides and G protein-coupled receptors that regulate feeding behavior. *Cell* **1998**, *92*, 573–585.
- (2) De Lecea, L.; Kilduff, T. S.; Peyron, C.; Gao, X.-B.; Foye, P. E.; Danielson, P. E.; Fukuhara, C.; Battenberg, E. L. F.; Gautvik, V. T.; Bartlett, F. S., II; Frankel, W. N.; Van Den Pol, A. N.; Bloom, F. E.; Gautvik, K. M.; Sutcliffe, J. G. The hypocretins: hypothalamus-specific peptides with neuroexcitatory activity. *Proc. Natl. Acad. Sci. U.S.A.* **1998**, *95*, 322–327.
- (3) Kukkonen, J. P. Physiology of the orexinergic/hypocretinergic system: a revisit in 2012. *Am. J. Physiol.: Cell Physiol.* **2013**, *304*, C2–32.
- (4) Zhang, X. Y.; Yu, L.; Zhuang, Q. X.; Zhu, J. N.; Wang, J. J. Central functions of the orexinergic system. *Neurosci. Bull.* **2013**, *29*, 355–365.
- (5) Tsujino, N.; Sakurai, T. Orexin/hypocretin: a neuropeptide at the interface of sleep, energy homeostasis, and reward system. *Pharmacol. Rev.* **2009**, *61*, 162–176.
- (6) Scammell, Th. E.; Winrow, Ch. J. Orexin receptors: pharmacology and therapeutic opportunities. *Annu. Rev. Pharmacol. Toxicol.* **2011**, *51*, 243–266.
- (7) Chemelli, R. M.; Willie, J. T.; Sinton, Ch. M.; Elmquist, J. K.; Scammell, T.; Lee, Ch.; Richardson, J. A.; Williams, S. C.; Xiong, Y.; Kisanuki, Y.; Fitch, T. E.; Nakazato, M.; Hammer, R. E.; Saper, C. B.; Yanagisawa, M. Narcolepsy in orexin knockout mice: molecular genetics of sleep regulation. *Cell* **1999**, *98*, 437–451.
- (8) Kalogiannis, M.; Grupke, S. L.; Potter, P. E.; Edwards, J. G.; Chemelli, R. M.; Kisanuki, Y. Y.; Yanagisawa, M.; Leonard, C. S. Narcoleptic orexin receptor knockout mice express enhanced cholinergic properties in laterodorsal tegmental neurons. *Eur. J. Neurosci.* **2010**, *32*, 130–142.
- (9) Morawska, M.; Buchi, M.; Fendt, M. Narcoleptic episodes in orexin-deficient mice are increased by both attractive and aversive odors. *Behav. Brain Res.* **2011**, *222*, 397–400.
- (10) Sakurai, T. Orexin deficiency and narcolepsy. *Curr. Opin. Neurobiol.* [Online early access]. DOI: <http://dx.doi.org/10.1016/j.conb.2013.04.007>. Published Online: May 7, 2013.
- (11) Lin, L.; Faraco, J.; Li, R.; Kadotani, H.; Rogers, W.; Lin, X.; Qiu, X.; De Jong, P. J.; Nishino, S.; Mignot, E. The sleep disorder canine narcolepsy is caused by a mutation in the hypocretin (orexin) receptor 2 gene. *Cell* **1999**, *98*, 365–376.
- (12) Thannickal, T. C.; Moore, R. Y.; Nienhuis, R.; Ramanathan, L.; Gulyani, S.; Aldrich, M.; Cornford, M.; Siegel, J. M. Reduced number of hypocretin neurons in human narcolepsy. *Neuron* **2000**, *27*, 469–474.
- (13) Nishino, S.; Ripley, B.; Overeem, S.; Lammers, G. J.; Mignot, E. Hypocretin (orexin) deficiency in human narcolepsy. *Lancet* **2000**, *355*, 39–40.
- (14) Hagan, J. J.; Leslie, R. A.; Patel, S.; Evans, M. L.; Wattam, T. A.; Holmes, S.; Benham, C. D.; Taylor, S. G.; Routledge, C.; Hemmati, P.; Munton, R. P.; Ashmeade, T. E.; Shah, A. S.; Hatcher, J. P.; Hatcher, P. D.; Jones, D. N.; Smith, M. L.; Piper, D. C.; Hunter, A. J.; Porter, R. A.; Upton, N. Orexin A activates locus coeruleus cell firing and increases arousal in the rat. *Proc. Natl. Acad. Sci. U.S.A.* **1999**, *96* (19), 10911–10916.
- (15) Lee, M. G.; Hassani, O. K.; Jones, B. E. Discharge of identified orexin/hypocretin neurons across the sleep–waking cycle. *J. Neurosci.* **2005**, *25*, 6716–6720.
- (16) Alam, M. N.; Gong, H.; Alam, T.; Jagannath, R.; McGinty, D.; Szymusiak, R. Sleep–waking discharge patterns of neurons recorded in the rat perifornical lateral hypothalamic area. *J. Physiol.* **2002**, *538*, 619–631.
- (17) Peyron, C.; Tighe, D. K.; van den Pol, A. N.; de Lecea, L.; Heller, H. C.; Sutcliffe, J. G.; Kilduff, T. S. Neurons containing hypocretin (orexin) project to multiple neuronal systems. *J. Neurosci.* **1998**, *18*, 9996–19915.
- (18) Gotter, A. L.; Roecker, A. J.; Hargreaves, R.; Coleman, P. J.; Winrow, C. J.; Renger, J. J. Orexin receptors as therapeutic drug targets. *Prog. Brain Res.* **2012**, *198*, 163–188.
- (19) Nishino, S. The hypocretin/orexin receptor: therapeutic prospective in sleep disorders. *Expert Opin. Invest. Drugs* **2007**, *16*, 1785–1797.
- (20) Coleman, P. J.; Cox, Ch. D.; Roecker, A. J. Discovery of dual orexin receptor antagonists (DORAs) for the treatment of insomnia. *Curr. Top. Med. Chem.* **2011**, *11*, 696–725.
- (21) Gatfield, J.; Brisbane-Roch, C.; Jenck, F.; Boss, Ch. Orexin receptor antagonists: a new concept in CNS disorders? *ChemMedChem* **2010**, *5*, 1197–1214.
- (22) Lebhod, T. P.; Bonaventura, P.; Shireman, B. T. Selective orexin receptor antagonists. *Bioorg. Med. Chem. Lett.* **2013**, *23*, 4761–4769.
- (23) Brisbane-Roch, C.; Dingemans, J.; Koberstein, R.; Hoefer, P.; Aissaoui, H.; Flores, S.; Mueller, C.; Nayler, O.; van Gerven, J.; de Haas, S. L.; Hess, P.; Qiu, C.; Buchmann, S.; Scherz, M.; Weller, T.; Fischli, W.; Clozel, M.; Jenck, F. Promotion of sleep by targeting the orexin system in rats, dogs and humans. *Nat. Med. (N.Y., NY, U.S.)* **2007**, *13*, 150–155.
- (24) Hoefer, P.; de Haas, S.; Winkler, J.; Schoemaker, R. C.; Chiossi, E.; van Gerven, J.; Dingemans, J. Orexin receptor antagonism, a new sleep-promoting paradigm: an ascending single-dose study with almorexant. *Clin. Pharmacol. Ther. (N.Y., NY, U.S.)* **2010**, *87*, 593–600.
- (25) Winrow, Ch. J.; Gotter, A. L.; Cox, Ch. D.; Doran, S. M.; Tannenbaum, P. L.; Breslin, M. J.; Garson, S. L.; Fox, S. V.; Harrell, Ch. M.; Stevens, J.; Reiss, D. R.; Cui, D.; Coleman, P. J.; Renger, J. J. Promotion of sleep by suvorexant—a novel dual orexin receptor antagonist. *J. Neurogenet.* **2011**, *25*, 52–61.
- (26) Bettica, P.; Nucci, G.; Pyke, C.; Squassante, L.; Zamuner, S.; Ratti, E.; Gomeni, R.; Alexander, R. Phase I studies on the safety, tolerability, pharmacokinetics and pharmacodynamics of SB-649868, a novel dual orexin receptor antagonist. *J. Psychopharmacol.* **2012**, *26*, 1058–1070.
- (27) Sun, H.; Kennedy, W. P.; Wilbraham, D.; Lewis, N.; Calder, N.; Li, X.; Ma, J.; Yee, K. L.; Ermlich, S.; Mangin, E.; Lines, C.; Rosen, L.; Chodakewitz, J.; Murphy, G. M. Effects of suvorexant, an orexin receptor antagonist, on sleep parameters as measured by polysomnography in healthy men. *Sleep* **2013**, *36* (2), 259–267.
- (28) Willie, J. T.; Chemelli, R. M.; Sinton, Ch. M.; Tokita, S.; Williams, S. C.; Kisanuki, Y. Y.; Marcus, J. N.; Lee, Ch.; Elmquist, J. K.; Kohlmeier, K. A.; Leonard, Ch. S.; Richardson, J. A.; Hammer, R. E.; Yanagisawa, M. Distinct narcolepsy syndromes in orexin receptor-2 and orexin null mice: molecular genetic dissection of non-REM and REM sleep regulatory processes. *Neuron* **2003**, *5*, 715–730.
- (29) Mang, G. M.; Duerst, Th.; Buerki, H.; Imobersteg, S.; Abramowski, D.; Schuepbach, E.; Hoyer, D.; Fendt, M.; Gee, Ch. E. The dual orexin receptor antagonist almorexant induces sleep and decreases orexin-induced locomotion by blocking orexin 2 receptors. *Sleep* **2012**, *35*, 1625–1635.
- (30) Gozzi, A.; Turrini, G.; Piccoli, L.; Massagrande, M.; Amantini, D.; Antolini, M.; Martinelli, P.; Cesari, N.; Montanari, D.; Tessari, M.; Corsi, M.; Bifone, A. Functional magnetic resonance imaging reveals different neural substrates for the effects of orexin-1 and orexin-2 receptor antagonists. *PLoS One* **2011**, *6*, e16406.
- (31) Dugovic, Ch.; Shelton, J. E.; Aluisio, L. E.; Fraser, I. C.; Jiang, X.; Sutton, S. W.; Bonaventura, P.; Yun, S.; Li, X.; Lord, B.; Dvorak, C. A.; Carruthers, N. I.; Lovenberg, T. W. Blockade of orexin-1 receptors attenuates orexin-2 receptor antagonism-induced sleep promotion in the rat. *J. Pharmacol. Exp. Ther.* **2009**, *330*, 142–151.
- (32) Kumrangal, B. A.; Kumar, D.; Mallick, H. N. Intracerebroventricular injection of orexin-2 receptor antagonist promotes REM sleep. *Behav. Brain Res.* **2013**, *237*, 59–62.

- (33) Steiner, M. A.; Gatfield, J.; Brisbane-Roch, C.; Dietrich, H.; Treiber, A.; Jenck, F.; Boss, Ch. Discovery and characterization of ACT-335827, an orally available, brain penetrant orexin receptor type 1 selective antagonist. *ChemMedChem* **2013**, *8*, 898–903.
- (34) Morairty, S. R.; Revel, F. G.; Malherbe, P.; Moreau, J. L.; Valladao, D.; Wettstein, J. G.; Kilduff, T. S.; Borroni, E. Dual hypocretin receptor antagonism is more effective for sleep promotion than antagonism of either receptor alone. *PLoS One* **2012**, *7*, e39131.
- (35) Smith, M. I.; Piper, D. C.; Duxon, M. S.; Upton, N. Evidence implicating a role for orexin-I receptor modulation of paradoxical sleep in the rat. *Neurosci. Lett.* **2003**, *341*, 256–258.
- (36) Mieda, M.; Hasegawa, E.; Kisanuki, Y. Y.; Sinton, C. M.; Yanagisawa, M.; Sakurai, T. Differential roles of orexin receptor-1 and -2 in the regulation of non-REM and REM sleep. *J. Neurosci.* **2011**, *31*, 6518–6526.
- (37) Chen, L.; McKenna, J. T.; Bolortuya, Y.; Winston, S.; Thakkar, M. M.; Basheer, R.; Brown, R. E.; McCarley, R. W. Knockdown of orexin type 1 receptor in rat locus coeruleus increases REM sleep during the dark period. *Eur. J. Neurosci.* **2010**, *32*, 1528–1536.
- (38) Di Fabio, R.; Pellacani, A.; Faedo, S.; Roth, A.; Piccoli, L.; Gerrard, P.; Porter, R. A.; Johnson, Ch. N.; Thewlis, K.; Donati, D.; Stasi, L.; Spada, S.; Stemp, G.; Nash, D.; Branch, C.; Kindon, L.; Massagrande, M.; Poffe, A.; Braggio, S.; Chiarparin, E.; Marchioro, C.; Ratti, E.; Corsi, M. Discovery process and pharmacological characterization of a novel dual orexin 1 and orexin 2 receptor antagonist useful for treatment of sleep disorders. *Bioorg. Med. Chem. Lett.* **2011**, *21*, 5562–5567.
- (39) Breslin, M. J.; Cox, Ch. D.; Whitman, D. B. Preparation of Diazaspirodecane Derivatives As Orexin Receptor Antagonists. PCT Int. Appl. WO 2007025069 A2 20070301, 2007.
- (40) A sulfonamide analogue of **1** was also used as starting point by a group at Takeda.⁴¹ In their series subtle structural changes had a surprising effect on selectivity and finally led to the identification of a compound with high in vitro selectivity for OX₂R. No in vivo data are reported.
- (41) Fujimoto, T.; Tomata, Y.; Kunimoto, J.; Hirozane, M.; Marui, S. Discovery of spiropiperidine-based potent and selective orexin-2 receptor antagonists. *Bioorg. Med. Chem. Lett.* **2011**, *21*, 6409–6413.
- (42) In order to calculate the amide rotational barrier, a coordinate scan has been performed using the relaxed coordinate scan tool contained in Jaguar (www.schrodinger.com). Default parameters have been used (density functional theory using the B3LYP functional). The amide torsion has been scanned from 0° to 180° using 20° steps.
- (43) Cox, Ch. D.; Breslin, M. J.; Whitman, D. B.; Schreier, J. D.; McGaughey, G. B.; Bogusky, M. J.; Roecker, A. J.; Mercer, S. P.; Bednar, R. A.; Lemaire, W.; Bruno, J. G.; Reiss, D. R.; Harrell, C. M.; Murphy, K. L.; Garson, S. L.; Doran, S. M.; Prueksaritanont, T.; Anderson, W. B.; Tang, C.; Roller, S.; Cabalu, T. D.; Cui, D.; Hartman, G. D.; Young, S. D.; Koblan, K. S.; Winrow, Ch. J.; Renger, J. J.; Coleman, P. J. Discovery of the dual orexin receptor antagonist [(7R)-4-(5-chloro-1,3-benzoxazol-2-yl)-7-methyl-1,4-diazepan-1-yl][5-methyl-2-(2H-1,2,3-triazol-2-yl)phenyl]methanone (MK-4305) for the treatment of insomnia. *J. Med. Chem.* **2010**, *53*, 5320–5332.
- (44) Cox, Ch. D.; McGaughey, G. B.; Bogusky, M. J.; Whitman, D. B.; Ball, R. G.; Winrow, Ch. J.; Renger, J. J.; Coleman, P. J. Conformational analysis of N,N-disubstituted-1,4-diazepane orexin receptor antagonists and implications for receptor binding. *Bioorg. Med. Chem. Lett.* **2009**, *19*, 2997–3001.
- (45) Coleman, P. J.; Schreier, J. D.; McGaughey, G. B.; Bogusky, M. J.; Cox, Ch. D.; Hartman, G. D.; Ball, R. G.; Harrell, C. M.; Reiss, D. R.; Prueksaritanont, Th.; Winrow, Ch. J.; Renger, J. J. Design and synthesis of conformationally constrained N,N-disubstituted 1,4-diazepanes as potent orexin receptor antagonists. *Bioorg. Med. Chem. Lett.* **2010**, *20*, 2311–2315.
- (46) Coleman, P. J.; Schreier, J. D.; Roecker, A. J.; Mercer, S. P.; McGaughey, G. B.; Cox, Ch. D.; Hartman, G. D.; Harrell, C. M.; Reiss, D. R.; Doran, S. M.; Garson, S. L.; Anderson, W. B.; Tang, C.; Prueksaritanont, Th.; Winrow, Ch. J.; Renger, J. J. Discovery of 3,9-diazabicyclo[4.2.1]nonanes as potent dual orexin receptor antagonists with sleep-promoting activity in the rat. *Bioorg. Med. Chem. Lett.* **2010**, *20*, 4201–4205.
- (47) Coleman, P. J.; Schreier, J. D.; Cox, Ch. D.; Breslin, M. J.; Whitman, D. B.; Bogusky, M. J.; McGaughey, G. B.; Bednar, R. A.; Lemaire, W.; Doran, S. M.; Fox, S. V.; Garson, S. L.; Gotter, A. L.; Harrell, C. M.; Reiss, D. R.; Cabalu, T. D.; Cui, D.; Prueksaritanont, Th.; Stevens, J.; Tannenbaum, P. L.; Ball, R. G.; Stellabott, J.; Young, S. D.; Hartman, G. D.; Winrow, Ch. J.; Renger, J. J. Discovery of [(2R,5R)-5-[[[(5-fluoropyridin-2-yl)oxy]methyl]-2-methylpiperidin-1-yl][5-methyl-2-(pyrimidin-2-yl)phenyl]methanone (MK-6096): a dual orexin receptor antagonist with potent sleep-promoting properties. *ChemMedChem* **2012**, *7*, 415–425.
- (48) Gracias, V.; Gasielki, A. F.; Moore, J. D.; Akritopoulou-Zanze, I.; Djuric, S. W. An expedient route to diaza-spirocycles utilizing a sequential multicomponent α -aminoallylation/ring-closing metathesis strategy. *Tetrahedron Lett.* **2006**, *47*, 8977–8980.
- (49) Leeson, P. D.; Springthorpe, B. The influence of drug-like concepts on decision-making in medicinal chemistry. *Nat. Rev. Drug Discovery* **2007**, *6* (11), 881–890.
- (50) Hopkins, A. L.; Groom, C. R.; Alex, A. Ligand efficiency: a useful metric for lead selection. *Drug Discovery Today* **2004**, *9* (10), 430–431.
- (51) In the literature suvorexant was reported to be a DORA for human, rat, and rhesus receptors,²¹ No data for the mouse receptors are published.
- (52) Maurer, T. S.; DeBartolo, D. B.; Tess, D. A.; Scott, D. O. Relationship between exposure and non-specific binding of thirty-three central nervous system drugs in mice. *Drug Metab. Dispos.* **2005**, *33*, 175–181.
- (53) Pack, A. I.; Galante, R. J.; Maislin, G.; Cater, J.; Metaxas, D.; Lu, S.; Zhang, L.; Von Smith, R.; Kay, T.; Lian, J.; Svenson, K.; Peters, L. L. Novel method for high-throughput phenotyping of sleep in mice. *Physiol. Genomics* **2007**, *28* (2), 232–238.
- (54) Herring, W. J.; Snyder, E.; Budd, K.; Hutzelmann, J.; Snavely, D.; Liu, K.; Lines, Ch.; Roth, T.; Michelson, D. Orexin receptor antagonism for treatment of insomnia – A randomized clinical trial of insomnia. *Neurology* **2012**, *79*, 2265–2274.
- (55) Bettica, P.; Squassante, L.; Groeger, J. A.; Gennery, B.; Winsky-Sommerer, R.; Dijk, D. J. Differential effects of a dual orexin receptor antagonist (SB-649868) and zolpidem on sleep initiation and consolidation, SWS, REM sleep, and EEG power spectra in a model of situational insomnia. *Neuropharmacology* **2012**, 1–10.
- (56) Faedo, S.; Perdon, E.; Antolini, M.; di Fabio, R.; Pich, E. M.; Corsi, M. Functional and binding kinetic studies make a distinction between OX₁ and OX₂ orexin receptor antagonists. *Eur. J. Pharmacol.* **2012**, *692*, 1–9.
- (57) Malherbe, P.; Borroni, E.; Pinard, E.; Wettstein, J. G.; Knoflach, F. Biochemical and electrophysiological characterization of almorexant, a dual orexin 1 receptor (OX₁)/orexin 2 receptor (OX₂) antagonist: comparison with selective OX₁ and OX₂ antagonists. *Mol. Pharmacol.* **2009**, *76*, 618–631.
- (58) Jiang, X.-H.; Song, Y.-L.; Long, Y.-Q. Facile synthesis of 4-substituted-4-aminopiperidine derivatives, the key building block of piperazine-based CCR5 antagonists. *Bioorg. Med. Chem. Lett.* **2004**, *14*, 3675–3678.
- (59) Badiger, S.; Behnke, D.; Betschart, C.; Chaudhari, V.; Costeta, S.; Hintermann, S.; Lerchner, A.; Limam, F.; Ofner, S.; Pandit, C.; Wagner, J. Di/tri-aza-spiro-C9-C11alkanes. US20120165331, 2012.